

ACDIS Research Report

Probability Distributions for Carbon Emissions and Atmospheric Response: Results and Methods

Clifford Singer, T. S. Gopi Rethinaraj, Samuel Addy, David Durham, Murat Isik, Tod Kaspar, Madhu Khanna, Brandon Kuehl, Janding Luo, Wilma Quimio, Kothavari Rajendran, Ji Qiang, Jürgen Scheffran, T. Nedjla Tiouririne, and Junli Zhang

Department of Nuclear, Plasma, and Radiological Engineering,

Department of Agricultural and Consumer Economics, and

Program in Arms Control, Disarmament, and International Security

University of Illinois at Urbana-Champaign

This publication is supported in part by a grant from the John D. and Catherine T. MacArthur Foundation and by funding from the University of Illinois. It is produced by the Program in Arms Control, Disarmament, and International Security at the University of Illinois at Urbana-Champaign.

The University of Illinois is an equal opportunity / affirmative action institution.

ACDIS Publication Series: *ACDIS Swords and Ploughshares* is the bulletin of ACDIS and publishes scholarly articles for a general audience. The *ACDIS Occasional Paper* series is the principal publication to circulate the research and analytical results of faculty and students associated with ACDIS. The *ACDIS Research Reports* series publishes technical reports and the results of grant and contract research. Publications of ACDIS are available upon request. For additional information consult the ACDIS home page on the World Wide Web at: <http://www.acdis.uiuc.edu/>

Published 2007 by ACDIS // ACDIS SIN:2.2007
University of Illinois at Urbana-Champaign
359 Armory Building, 505 E. Armory Ave.
Champaign, IL 61820-6237

Series editor: Matthew A. Rosenstein

Note: a later version of this paper appears in the journal *Climatic Change*, vol. 88 nos. 3-4 (June 2008), and can be accessed at:

<http://dx.doi.org/10.1007/s10584-008-9410-4>

PROBABILITY DISTRIBUTIONS FOR CARBON EMISSIONS
AND ATMOSPHERIC RESPONSE: RESULTS AND METHODS

CLIFFORD E. SINGER, T.S. GOPI RETHINARAJ, SAMUEL ADDY,
DAVID DURHAM, MURAT ISIK, MADHU KHANNA, BRANDON KUEHL,
JIANDING LUO, WILMA QUIMIO, KOTHAVARI RAJENDRAN, DONNA
RAMIREZ, JI QIANG, JÜRGEN SCHEFFRAN, T. NEDJLA TIOURIRINE,
and JUNLI ZHANG

*University of Illinois at Urbana-Champaign
Program in Arms Control, Disarmament and International Security,
Champaign, IL 61820, USA
217-244-0218; 217-244-5157 (fax); E-mail: csinger@uiuc.edu*

Abstract. Probability distributions for carbon burning, atmospheric CO₂, and global average temperature are produced by time series calibration of models of utility optimization and carbon and heat balance using log-linear production functions. Population growth is used to calibrate a logistically evolving index of development that influences production efficiency. Energy production efficiency also includes a coefficient that decreases linearly with decreasing carbon intensity of energy production. This carbon intensity is a piecewise linear function of fossil carbon depletion. That function is calibrated against historical data and extrapolated by sampling a set of hypotheses about the impact on the carbon intensity of energy production of depleting fluid fossil fuel resources and increasing cumulative carbon emissions. Atmospheric carbon balance is determined by a first order differential equation with carbon use rates and cumulative carbon use as drivers. Atmospheric CO₂ is a driver in a similar heat balance. Periodic corrections are included where required to make residuals between data and model results indistinguishable from independently and identically distributed normal distributions according to statistical tests on finite Fourier power spectrum amplitudes and nearest neighbor correlations. Asymptotic approach to a sustainable non-fossil energy production is followed for a global disaggregation into a tropical/developing and temperate/more-developed region. The increase in the uncertainty of global average temperature increases nearly quadratically with the increase in the temperature from the present through the next two centuries.

1. Introduction

Uncertainty about how fossil carbon use will drive global climate change complicates many aspects of long-term land use planning at the regional and national levels around the world. There is thus considerable interest in probability distributions for the actual outcome (c.f. Giorgi and Francisco, 2000; Andronova and Schlesinger, 2001; Forest et al., 2002; Webster et al., 2002; Dessai and Hulme, 2003; Dessai and Hulme, 2004; Mastrandrea and Schneider, 2004; Murphy et al., 2004; Richels et al., 2004; Kriegler, 2005; Giorgi, 2005; Stainforth et al., 2005). There has been a particular emphasis in very recent literature on developing probability distributions for climate response to emissions scenarios (Collins et al., 2006; Dettinger, 2006; Greene et al., 2006; Raisanen and Ruokolainen, 2006). Accomplishing this in a way that is systematically connected to time-series data has long been known to be a challenging exercise (c.f. Chapter 5 of Nordhaus, 1994). Probability distributions rather than definitive predictions are the best that can be expected, given uncertainties in the future of carbon use and atmospheric response. An alternate approach is to bracket the most likely actual outcome with scenarios such as “business as usual” vs. “optimal response” with the aim of contrasting the possible benefits of international cooperation on limiting atmospheric carbon accumulation with the dangers of failing to do so. Such scenario building requires self consistent models, but not necessarily the type of systematic statistical analysis undertaken here to support outcome probability distributions.

With respect to the impact of uncertainties about future greenhouse gas emissions, an ambitious previous effort at estimating “uncertainty in emissions projections for climate models” is described in paper of that title by Webster et al. (2002). That work explores the implications of uncertainties about a measure of the energy intensity of economic production, productivity growth, and seven classes of greenhouse gases, for twelve different geographical regions. In that case probability distributions for the values of the macroeconomic parameters were obtained by surveys of expert assessment rather than directly by time-series analysis using historical data. Desai and Hulme (2004) subsequently uniformly sampled carbon emissions scenarios to support calculation of cumulative probability distributions for changes in global average temperature. Richels et al. (2004) nonuniformly sampled a similar set of scenarios towards much the same end. Also relying on a survey of expert opinion, Mastrandrea and Schneider (2004) aimed at a probabilistic assessment similar to that done in the present paper. Their work references the original DICE model (Nordhaus, 1992). In that model all capital and labor is assigned to a single GDP production function in a globally aggregated model, and the carbon intensity of energy production is an assigned function of time rather than a function of cumulative carbon use.

The work described in the present paper illustrates a different method to complement the samplings of expert input used in the above-mentioned studies. The method described here uses time-series data to calibrate probability distributions for global average temperature change based on econometric and

physical models of the use of fossil carbon and its influence on the atmosphere. The primary emphasis is on carbon emissions econometrics, with very simple atmospheric carbon and heat balance models appended merely to illustrate the use of the more complete econometric results. Thus the probability distributions developed here for global average temperature increase do not include a large number of a priori uncertain parameters found in more complete analyses. The result is that range of atmospheric carbon and global average temperatures in the central ninety-five centiles of random samples found here is expected to be a lower bound on what a more complete study using the same type of methodology would produce.

Time-series analysis is used here because this is needed for data to constrain model projection probabilities in the most useful way (c.f. Verbecke and De Clercq, 2006). The reason for this is that historical time series reveal deeply ingrained patterns in the evolution of economic production and energy use that seem to have been difficult to dislodge except through rare and major socioeconomic transformations. Examples of such major transformations are the transition to lower mortality and fertility rates and the widespread use of fossil fuels that followed the Napoleonic Wars and the invention of an efficient steam engine. Deeply ingrained patterns of economic development are evident in plots of the nearly two orders of magnitude increase in per capita gross domestic product (GDP) on a logarithmic scale versus time from 1870 (as on pp. 333–334 in Barro and Sala-i-Martin, 1995). Persistent patterns are also evident on a shorter but still significant timescale on the plots of carbon intensity of energy use versus cumulative fossil carbon use shown below in Figure 4.

An alternative sometimes used to avoid systematic calibration against longer time series is constraining models to match values and rates of change of observations near a single recent reference time. This approach can be useful for scenario building. However this simpler “point and slope” approach does not make full use of data available for constraint of probability distributions for model parameters. This is particularly the case when there are periodic oscillations around background evolutionary trends, as in some of the data sets used here. In cases where periodic variations around background trends are important, e.g. as is well known to be the case for GDP over business cycles, extrapolation results can vary considerably when time-rates-of-change over shorter intervals are used instead of calibration against extended time-series data for setting modeling parameters.

If the theoretical framework chosen is robust enough and the data management is sufficiently flexible, as is the case here, then it should be possible to generalize the kind of top-level analysis done here to greater levels of disaggregation and longer time spans without moving outside the range of applicability. To this end a dynamic utility optimization approach is used that is somewhat similar to that of Manne and colleagues (Manne et al., 1995; Manne, 2006), following on from Nordhaus (1993 and 1994) and Tol (1994). The potential advantages of systematically calibrating and sampling probability distributions for essentially all of the parameters in a model when extrapolating future energy use and carbon emissions is counterbalanced by the considerable difficulty

of doing this in such a way that the residuals between the results of the model and an extensive data set are consistent with a tractable statistical model. To make this more manageable within the scope of the present study, only two economic production sectors in two grouped sets of countries are included, as described in detail below. However, the solution approach used is unrestricted in the time period it can cover and the time resolution that can be efficiently obtained. Moreover, the economic model used has been formulated in a way that can readily be generalized to include more detail on production sectors, and database construction and data aggregation methods have been developed so that any desired sets of countries can automatically be grouped together for analysis.

The data used include annual estimates of population and GDP for 1950–2001 from Maddison (2001). Also used are time series for 1950–2001 from the United Nations for nine different energy sources (UNSD, 2005) from 220 different geographic areas. PERL language coding for extracting the required information from the UN database is included in CD-ROM format in a PhD thesis by Rethinaraj (2005). These energy sources include fossil fuels in the forms of coal, oil, natural gas. They also include the fossil fuel energy equivalent of electrical power at a reference thirty-eight percent thermal to electric conversion efficiency for use of hydropower, geothermal energy, tides, nuclear energy, wind, and solar thermal energy to generate electricity. The range of data used and the number of years each type is averaged over are indicated by the data points on the figures given below. Carbon released to the atmosphere per exajoule of energy obtained from burning coal is estimated at 0.0255 billion metric tonnes (Gtonne). Oil and natural gas are estimated respectively to release 0.745 and 0.54 times as much carbon per unit energy as coal. For fitting data on carbon intensity of energy production as a function of cumulative carbon use, estimates of the use of coal, oil, and natural gas before 1950 are needed. From 1925 through 1949 these are taken from Darmstadter (1971). Earlier data are from Mitchell (2003) and from Etemad and Luciani (1991), drawing on the electronic formatting of Goldewijk (2004). Time-series data for atmospheric carbon dioxide are from Keeling and Whorf (2004) and for global average temperature from Jones et al. (2001). A more complete description of the methods used for extracting and regionally aggregating the data is available as a research report in electronic format (Rethinaraj, 2005).

To facilitate generalization of the present approach to more complete analyses, a particular goal is transparency of the formulas and methods used. An overview of the approach used is given in the following few paragraphs, and details are provided in the subsequent sections of the main text and in the Appendix section.

Subject to the constraint of an overall evolving total labor supply, labor and capital are dynamically allocated to primary energy and final consumables production and investment in order to maximize the total time-integrated discounted utility of per capita consumption. The efficiency of primary energy production depends on the amount of carbon consumed per unit of primary en-

ergy production (hereafter “carbon intensity”), and primary energy production is an essential input to increases in overall economic production.

For the examples shown here, only two aggregate regions are used. These include a “temperate and more developed” region and a “tropical/developing” region. The temperate region includes all UN geographical data units any part of which lies poleward of forty degrees latitude. (This includes all separately administered portions of China and Korea, and Puerto Rico with the United States). Everything else is in what for brevity is called the tropical region. With this division a simple logistic model of the growth of populations over their pre-industrial base levels is remarkably adequate.

It is useful to note that increasing levels of economic development broadly correlate with decrease in population growth rates, at least at the level of aggregation used here. Thus the ratio of industrial era population increment to its long-term limit value gives a unit logistic function that can be used as an index of economic production efficiency. Labor supply is of course also connected to population, with a simple proportionality assumed here.

In this work the same type of formulation is used for the more developed and developing region. This formulation allows the data rather than an a priori assumption to determine the ratio of the long-term-limit values of per capita GDP and per capita energy use. In the context of this approach, per capita GDP and per capita energy use are conditionally convergent, in that they can be modeled with the same type of formulas. However, since the time-series-calibrated long-term limit values of per capita GDP and per capita energy are much smaller for the developing region than for the more developed region, there is not even close to absolute convergence of these economic indicators for the two regions.

To analyze economic production, for each region overall economic production efficiency is taken to be log-linear in a development index and in labor, capital, and primary energy input. Primary energy production is also taken to be log-linear in this index and in labor and capital applied to energy production. Primary energy production efficiency for each region also includes a factor that depends linearly on the cumulative use of fossil carbon in that region. This additional energy production efficiency factor reflects the dependence on cumulative fossil carbon use of both the depletion of more readily extractable fossil fuels and the effect of accumulating local and regional experience with diseconomies of fossil fuel use. These choices approach the minimally complex dynamic optimization model that can deal with the impacts of population growth and saturation as well as the inevitable eventual transition from fossil-dominant to non-fossil primary energy production.

The principal motivation here for minimizing complexity is to construct a model that can tractably be subjected to a complete data-constrained calibration of outcome probabilities. To this end it has proven very convenient to be able to construct analytic solutions based on expansions in three small parameters. These are referred to here as the capital fraction of energy production, the (dimensionless) fossil carbon depletion rate, and the (dimensionless) “capitalization lag.” Primary energy production consumes at most a few percent of

global GDP, so the capital fraction of energy is an excellent expansion parameter. (Based on prices and use data from the U.S. Energy Information Agency, primary energy production as operationally defined below for the purposes of this study, can be estimated as having been less than three percent of global GDP in 2002). It also turns out to be sufficient to retain only the lowest order terms in an expansion in the fossil depletion rate, as described below.

The capitalization lag is the fractional amount by which capital accumulation differs from the value it would have if labor supply and production efficiency were frozen and the economy allowed to relax to equilibrium. The computations reported here are carried out through first order in the capitalization lag. Second order corrections are calculated only to examine the size of the omitted terms.

Systematically calibrating and sampling probability distributions for extrapolating a non-linear model of carbon emissions rates requires spanning the multidimensional parameter space of a priori uncertain model inputs through selection of a large number of random samples. This is the primary reason that we have chosen a set of equations and an expansion method that produces analytic solutions, rather than going through the extra step of fitting analytic functions to the input-output relations of more computationally expensive models (as in Webster et al., 2002). Within this constraint, we have based the model on some of the same principles used elsewhere, particularly in the approach that underlies continuing studies using the MERGE models (Manne, 2006), but with finer time resolution. Compared to current versions of MERGE, missing from the present approach are breakdown of both carbon burning and non-fossil energy use into electrical and other primary energy sectors. Also neglected here are shipments of fossil fuels between regions and payments therefor. Such interactions between regions are neglected largely for computational convenience, but also because the level of aggregation is so large that, for example, carbon consumption in the temperate region is largely in the form of coal, natural gas, and also still substantial amounts of oil extracted within that region. The current approach also lacks the very detailed energy sector analysis integrated with the overall economy in models such as NEMS, MARKAL-MACRO, NEMO, and AMIGA (c.f. Worrell et al., 2004). The systematic time-series calibration and sampling of probability distributions including such important refinements could be approached by sampling a tractable subset of the parameters that have the most influence on the results from more computationally complex models. Alternatively or additionally, the present approach is formulated so that it can readily be generalized and solved computationally to the same end. Either approach is a challenging exercise that lies beyond the scope of the present work, which itself is sufficiently involved that a compact albeit reasonably complete description is all that can be managed here.

Another important limitation of the results presented here for carbon emissions is that they are based simply on extrapolations of historical trends, with the one important exception of how possibilities for future carbon intensities of energy production are sampled to project beyond the time period covered by mere extrapolation of historical calibrated results. Other than this, there is no allowance for technological or policy changes that precipitate a substantial de-

parture from historical trends. (Examples could include genetically engineered biomass production that dramatically reduces the use of fossil fuels, or a global consensus that reduces proliferation and safety concerns and leads to substantial reduction in impediments to siting nuclear power plants and costs of related waste management facilities.) Moreover, there is a simple logistic-to-a-power evolution of overall production efficiency (the amount of GDP for a given input of labor, capital, and energy applied to everything but primary energy production). The inputs into GDP are extrapolated smoothly into the future, accounting for multiple-period periodic variations but not for singular events such as the world wars and global pandemics that occurred before the data range used for time-series calibration of the probability distribution functions for sampled parameters. The type of sampling procedure used here for extrapolation of the carbon intensity of energy production could be extended to sample uncertainties in future carbon emissions due to an inferred probability distribution of such disruptions. This would require numerical integration of underlying equations, which is a manageable but more computationally intensive approach (Zhang, 2000). To the extent that sampling of potentially important uncertainties has been omitted here, a more general approach to such matters would be expected to produce a broader range of results than shown here in this simpler illustrative example of the methodology.

For extrapolations into the future based on fits to historical time series there is a question of how long the functional forms used to fit past behavior will remain appropriate. In the present study, this question arises most obviously for the dependence of the carbon intensities of energy production on cumulative fossil carbon use. We operationally define primary energy as the sum of the thermal energy equivalent from use of coal, oil, natural gas, and electricity production from nuclear, hydro, tidal, geothermal, wind, and solar thermal sources. This includes only energy sources that are generally sold to consumers rather than being used locally, both because these are most readily measureable and because they have historically either produced carbon emissions or competed directly with fossil fuels (in the case of non-fossil centrally generated electricity). Thus, care should be taken in comparing the results presented here with other projections of future energy use that have a broader operational definition of what is included in energy use. In the present approach, advances in photovoltaics and non-electricity-production use of solar and geothermal energy are operationally treated as equivalent to conservation since these energy sources are often used locally. The primary energy input to biofuels production is included in the primary energy sector. However, biofuels themselves are a secondary form of energy included in the rest of the economy, and any net solar energy input to them is treated as equivalent to an increase in the primary energy efficiency of production that is calibrated against time-series data. Pre-industrial energy sources other than coal are taken here to be adequate to sustain pre-industrial base level economic production and populations. These various conventions focus attention on the role of energy sources historically relied upon for industrial-era increments in GDP.

Using a standard carbon/energy content ratio for each of the fossil energy sources described above, time-series data on the use of all of the included primary energy sources is converted into time-series data on carbon intensity (Rethinaraj, 2005). Historically, the dependence of carbon intensity on cumulative fossil carbon use in each region can be well fit with a piecewise linear function. The linear segments are separated approximately by the first drilling for oil, the culmination of the global spread of colonialism and World War I, World War II, and the emergence of the Organization of Petroleum Exporting Countries cartel (OPEC). Before the first use of oil, in this approximation the carbon intensity is the reference value for coal of 0.0255 billion (metric) tonnes per 10^{18} Joule (GT/EJ). After the historical “age of coal,” the carbon intensity decreased to an average of 0.74–0.75 times that of coal, which is very close to the corresponding reference ratio 0.745 for oil. At this point there were breaks in the slope of carbon intensity plotted vs. cumulative carbon use.

The historical age of coal was succeeded by an era in which fluid fossil fuels (oil and natural gas) are the dominant primary energy source. However, the decline in carbon intensity might be expected to level off when the carbon intensity is about 0.54 times the level for coal, which is the carbon intensity of natural gas. This level can likely be reached by substituting in the somewhat larger resources for natural gas than oil at comparable production costs per unit energy content, and balancing remaining coal and oil with a modest complement of non-fossil primary energy sources. However, the resulting rapid depletion of conventional natural gas resources would tend to produce a back-substitution of coal for natural gas (c.f. EIA, 2005), even as the use of non-fossil energy sources may continue to increase. Here we do not make a unique assumption about what carbon intensity of energy production will have to be reached before the historical rate of its decrease with cumulative carbon use is changed, or about what will happen thereafter. Rather, as illuminated graphically below in Figure 8, we sample a probability distribution for the point at which the slope of a plot of carbon intensity of energy production versus cumulative carbon use changes. We also sample a probability distribution for the change in this slope thereafter. This reduced absolute value of the slope is hypothesized to continue until there is an effective international understanding that imposes substantial carbon taxes or other methods of limiting coal consumption in order to move out of this “new age of coal.”

The hypothesis investigated here is that an understanding on accelerating the decline of carbon intensity of energy production with cumulative carbon will start to be more effectively implemented when cumulative emissions have exceeded an as yet imprecisely known level. For the purposes of illustration, this level is sampled from a probability distribution centered on an estimate by Petschel-Held et al. (1999) of cumulative carbon emissions that produce a global average temperature industrial age increment of 2°C . This choice is motivated by the inference that exceeding this level of global average temperature increase is expected to produce noticeable and deleterious effects not only in the tropical region but also increasingly in the temperate one as well (c.f. Keller et al., 2005, and Kypreos, 2006). This approach provides a computationally

convenient method of allowing each sampled result to react to its own evolution of cumulative carbon emissions. Other than this, there is no feedback of climate change resulting from carbon emissions included in the present analysis.

We implicitly assume that the effect on GDP of climate change resulting from the calculated carbon emissions at various times is smaller than or comparable to the order of magnitude of the capital fraction of energy production. Then the economic impact of climate change can also be neglected to lowest order, in an expansion in the capital fraction of energy, when estimating the evolution of capital and labor applied to other than primary energy production. For the historical period used for time-series calibration, this seems clear enough. This leaves the question whether and when the primary energy production sector will be more directly influenced by the effects of carbon emissions, rather than indirectly through their overall effect on GDP and thus the portion thereof available for capital investment in the energy sector. In the present approach direct “order one” effects of carbon emissions on energy production are expressed through the formula used for carbon intensity of energy production. To the extent that concerns about global effects of carbon emissions already influenced energy production decisions during the historical calibration period, this influence is reflected in the data-calibrated slope of the decline of carbon intensity of energy production with cumulative fossil carbon use as shown in Figure 4 below. To the extent that this influence may change in the future in ways not captured by extrapolation of this calibration against historical data, in the present approach this change is reflected by sampling probability distributions based on the hypotheses about this slope just discussed above and illustrated below in Figure 8.

The approach used here to possible future departures from systematically calibrated and sampled extrapolations of the historical decline in the carbon intensity of energy production with cumulative fossil carbon use has advantages and disadvantages. Advantages are that it is simple to sample the probability distributions used. It is also straightforward to relate them to two reasonably likely future developments. One of these is that it may become increasingly expensive on the production side to reduce carbon intensity of primary energy below the level reached when the rate of use of natural gas overtakes that of oil and coal, with a balance between the latter and non-fossil energy sources that leads to an overall carbon intensity of energy production comparable to that for natural gas. The other reasonably likely development is that the incentive to more rapidly decrease the carbon intensity of energy production will increase as cumulative carbon emissions lead to a situation where the deleterious effects of increased atmospheric carbon concentration are more visibly apparent in temperate as well as tropical region countries. A disadvantage is that this approach is not the result of the application of a data-calibrated theory of how developments in technology and decision making by private and public bodies interact to influence decisions between different energy sources—important topics but beyond the scope of the present analysis.

It should be emphasized that the approach used here to extrapolating the carbon intensity of energy production does not assume a complete absence of

effective near-term action on reducing carbon emissions both among selected countries and at the sub-national level. Indeed, concern about the global environmental effects of carbon emissions may well be part of what continues to drive down the carbon intensity of primary energy production along the historical trend line for some time into the future. Rather, we simply allow for a likelihood that there will be a temporary reduction in the rate of decline of carbon intensity of energy production with cumulative carbon use somewhere around the point where it can not so easily be reduced by substituting in less carbon intensive fossil fuels and making marginal increases in the proportion of capital-intensive non-fossil energy sources.

The models of atmospheric response to carbon emissions used here are simple first order differential equations that can be converted to integrals over driving terms. The driving terms for atmospheric carbon loading are the fossil carbon emissions rate and cumulative fossil carbon burning. The driving term for the atmospheric heat balance equation is a suitable function of atmospheric carbon loading. For simplicity, no additional heat balance driving terms are included, so the present results should be viewed as merely illustrative of the uncertainties obtained when only the recently and future dominant driving term of fossil carbon use is accounted for. Integrations over historical time series for the driving terms allow the development of model parameters' posterior probability distributions. These distributions are randomly sampled to provide a set of future atmospheric response extrapolations.

A plethora of potentially significant contributions to overall atmospheric heat balance that are not treated in the simple model used here include changes in other well-mixed greenhouse gases, stratospheric H₂O, ozone, snow albedo, cloud cover, solar irradiance, and aerosols. If the net contribution of these is modest compared to that from changes in atmospheric CO₂ (as in Hansen et al., 2006), and fossil fuel burning dominates these changes, then the maximum likelihood extrapolation of the very simple model for global average temperatures used here may be a reasonable indication of response to the extrapolated carbon emissions. However, sampling probability distributions for each of these other effects should noticeably increase the spread of the extrapolated global average temperatures (e.g. as in Andronova and Schlesinger, 2001, or Murphy et al., 2004). Without the need for sampling a large number of input parameters and doing many runs of more computationally demanding models, the probability distributions developed for the much simpler model used in this paper serve the basic purpose here. This purpose is to simply illustrate that uncertainties in the atmospheric heat balance make the largest contribution to overall spread in extrapolations of global average temperature within the context of the approach to extrapolation of carbon emissions used here.

Probability distributions for all but two parameters used to model historical time series are determined by data sets without the need for informative prior probability distributions. One of these exceptions is the ratio, in the limit of mature technologies, of energy production efficiency using non-fossil fuels to that using essentially undepleted fossil fuels. Based on the spread of busbar electricity prices at various delivered fuel prices and the trade-off between capital

and fuel costs in internal combustion engine fuel efficiency, a log-normal prior probability distribution centered on a value of 2 is used for this parameter. A log-normal prior probability distribution is also used for the coefficient of the rate of relaxation of global average temperature toward its pre-industrial base value. While both of these prior probability distributions can be estimated on the basis of physical systems analysis independently of time-series data, there is incomplete precision concerning the appropriate standard deviations for their prior probability distributions. A plausible range of these prior uncertainties is thus covered by reporting results based on three different values for their standard deviations.

From this introductory discussion, it should be abundantly clear that the objectives of the present paper are limited ones. These are to give an explicit description of a methodology for sampling calibrating probability distributions for model parameters systematically calibrated against historical time-series data, and to demonstrate the minimum range of outcomes from extrapolating models of this type. To quote from a complementary study, concerning the spread in the outcomes “we do not recommend that our quantitative results be taken literally, but we suggest that our probabilistic framework and methods be taken seriously” (Mastrandrea and Schneider, 2004).

Based on the above considerations, the rest of this paper proceeds as follows. The next section presents the equations used, maximum likelihood estimates of their adjustable parameters, and comparisons of the results with historical time-series data. The succeeding two sections outline methods and results for sampling probability distributions for these parameters. An interesting result is the approximately quadratic growth over a long time span of the uncertainty of temperature increase with the size of the temperature increase. The contributions of uncertainties in carbon emissions, atmospheric carbon balance, and atmospheric heat balance are then described. The result of this investigation is that uncertainties in the atmospheric heat balance model are predominant within the context of the formulas and data sets used here. Throughout this discussion it is implicit, without further repetition, that stated conclusions are drawn only within the context of the assumptions contained in the model formulation!

2. Maximum Likelihood and Sampled Fits for Carbon Use

For each geographical aggregation of data used here, we maximize the total time-integrated discounted utility of per capita consumption. Population is taken to be proportional to a development index a which evolves logistically from 0 to 1. Utility is taken to be a constant power of per capita consumption, its discount rate (the pure time rate of preference) is taken to be a constant ρ . Solving Euler-Lagrange equations derived from any constant times an integral to be maximized also maximizes the integral. Thus we can include a convenient constant factor in the denominator and extremize

$$\int_t^\infty dt a e^{-\rho t} (C/a)^{1-\theta} / (1-\theta)$$

Here consumption C is divided by a to make it proportional to per capita consumption, and the per capita utility is multiplied by a to make it proportional to the total per capita utility added up over the entire population. Consumption is final product yield less investment to make up for the sum of depreciation rK of total capital K and the rate $\dot{K} = dK/dt$ of its buildup. Throughout this discussion, over-barred and hatted quantities are dimensional constants, tilded quantities are dimensional and vary in time, and other quantities are generally dimensionless. Lists of symbols and their meanings are given in Tables A.1–A.6 in the Appendix. Some of the quantities in Tables A.2–A.4 and A.6 are not dimensionless. For symbols restricted uniquely to representing quantities having particular units, those units are also listed in these tables.

Units of time for dimensionless parameters are the “capitalization time” $\bar{t} = 1/(\bar{r} + \bar{\rho})$. Thus the dimensionless depreciation rate r in the above equation is $\bar{r}\bar{t}$, the dimensionless pure rate of time preference is $\rho = \bar{\rho}\bar{t}$, and these time units are mathematically convenient because they make $r + \rho = 1$. The overdot represents rate of change with respect to time when time is measured in units of \bar{t} . Dimensionless capital is measured in units of its long term limit value for each region, and consumption and production are measured in units of the ratio of this limit capital to \bar{t} .

To simplify the integral extremization results, final gross domestic production per unit time is represented as Y/α where the above-mentioned log-linear expression is $Y = [a^n((1 - \beta k)K)^\alpha((1 - \beta l)a)^\omega]^\varphi w^\beta$. Here βk and βl are the fractions of capital and labor applied to energy production $w = pa^\zeta(kK)^\alpha(la)^\omega$, where w is measured in units of its long-term limit value \bar{w} . Assuming $\alpha + \omega = \beta + \varphi = 1$, total production has constant returns to labor, capital, and energy input (in that multiplying each by the same constant multiplies overall production by the same constant). Energy production also has constant returns to scale with respect to capital and labor. For a given stage of development, energy production efficiency $p = 1 + (h - 1)f$ is taken to decrease linearly from an initial value h to limit value of 1 with the decrease in dimensionless carbon intensity f from an initial value of 1 (for coal only as a primary energy source) to approach a limiting value of 0 (with only non-fossil energy sources). From the equation $p = 1 + (h - 1)f$ it can be seen that, for a given value of the development index, the parameter h is the ratio of energy sector productivity with maximum (all coal) versus zero carbon use per unit energy production, i.e. for short the “fossil/non-fossil productivity” ratio. As noted above, we use a piecewise linear approximation to the dependence of f on cumulative fossil carbon use u . The above integral is maximized subject to the constraint that the rate of depletion of fossil carbon is equal to its rate of use for primary energy production.

As noted for example by Sachs (2005, p. 65), there tends to be a correlation between higher levels of economic productivity and lower population growth rates. While this is a correlation rather than a precise relationship, for appropriate levels of regional aggregation it leads to a convenient method for calibrating the development index a used here. We note that for population proportional to a logistic function a , the population growth rate is $\dot{a}/a = \nu(1 - a) = \nu z$

where $\nu = \bar{\nu}\bar{t}$ is a dimensionless constant. In terms of dimensional variables and constants, this equation is $d \ln[a]/d\bar{t} = \bar{\nu}z$ where $z = 1 - a$ is the “need for development” and $a = 1/(1 + \exp[-\nu t]) = 1/(1 + \exp[-\bar{\nu}(\bar{t} - \bar{t}_0)])$. The constants $\bar{\nu}$ and \bar{t}_0 are estimated using time-series data for the population growth rate $d \ln[a]/d\bar{t}$.

It should be kept in mind that utility optimization in this approach occurs only by adjusting allocations of available labor and capital to energy and other production sectors for a given level of social and technological development. Thus it is not assumed that resources are always optimally used, for example by promptly removing social barriers to more efficient use of energy or capital. Rather, resource use only becomes more closely optimal as the level of development “bootstraps” itself to approach the maximum achievable limit according to the equation $\dot{a} = \nu a(1 - a)$. Thus, the present approach is qualitatively consistent both with the observation that economies do not generally take full advantage of potential opportunities to maximize utility, and that they nevertheless can allocate capital and labor to recover from major disruptions on about the capitalization time independently inferred from other data in the present analysis (c.f. Barro and Sala-i-Martin, 1995, Section 10.2).

Expansion in three types of small parameters provides a convenient basis for the reduction of our utility maximization problem to analytic results. One of these is β , the “capital fraction of energy.” Another is the set of the constants ϵ_k in the fossil carbon balance equation. This equation takes the form $\dot{u} = \epsilon_k f w$ when time and energy use rates are expressed respectively in units of \bar{t} and \bar{w} and cumulative fossil carbon use u is expressed in units of the asymptotic limit amount of carbon ever used. In these units there is a different constant ϵ_k for each of the portions of the piecewise linear function used for the carbon intensity of energy use f as a function of u . This includes the portions $k = 2 \dots 5$ corresponding to the historical periods in which f decreases with u (i.e. after the first drilling for oil) and to $k = 5 \dots 7$ for the future, with f tending asymptotically to zero with time for $k = 7$. (The line segment corresponding to $k = 5$ partly covers the past and partly the future.) The third expansion parameter used is of order ν , the dimensionless initial population and development growth rate for each region. Details on the expansion in these parameters are given in the Appendix and in Rethinaraj (2005). Keeping terms to lowest order in β and ϵ_k for $k > 1$ and through first order in ν and expressing the results in dimensional form, the result for the rates of fossil carbon use is

$$\tilde{E} = \bar{E} a^\psi f p F_1^{\alpha/\omega} \text{ where } F_1 = (1 + a\delta)/(1 + \delta) \text{ and } \delta = \nu\theta\xi \text{ with } \xi = \eta/\omega$$

Here the constants \bar{E} (in GT/yr) and the exponents $\psi = 1 + \zeta + \alpha\xi$ are calibrated against time-series data for fossil carbon use from each region. The constants ξ are calibrated against the rate of growth per capita gross domestic product with development, given by $d \ln \bar{G}_{\text{DP}}/d \ln a = \xi + (\alpha/\omega)d \ln F_1/da$. (Here the values of \bar{G}_{DP} used are increments over 1820 base values, for the reasons outlined below in the discussion accompanying Figure 1.) To accomplish this calibration requires estimates of the capital fraction of production $\alpha = 1 - \omega$. It also requires

estimates of the constants θ and $\bar{t}=1/(\bar{r}+\bar{\rho})$ to obtain the capitalization lag $\delta = \bar{v}\bar{t}\theta\xi$ in the lag function $F_1 = (1 + a\delta)/(1 + \delta)$.

The required numbers $\alpha = 1 - \omega$, θ , \bar{r} , and $\bar{\rho}$ are assumed for simplicity to be universal constants and are estimated from various types of data in the literature, as described in the Appendix. A probability distribution for each of the four constants in the set $\{\alpha, \theta, \bar{r}, \bar{\rho}\}$ has been derived, with the results shown as the first four set sets of values in Table I. The resulting derived estimate for $\bar{t} = 1/(\bar{r} + \bar{\rho})$ is given at the bottom of Table I.

TABLE I

Global parameters

Value V	$\Delta V/V$	Type	Meaning
0.325	0.33	$0 < \alpha < 1$	capital share α
1.345	0.10	39	39 degrees of freedom for θ
0.107	0.06	28	depreciation rate \bar{r} in 1/yr
0.022	0.08	weighted	discount rate $\bar{\rho}$ in 1/yr
0.422	0.13	29	tropical productivity parameter ξ
0.978	0.13	33	temperate parameter ξ
7.76		derived	capitalization time \bar{t} , yr

An estimate for the GDP productivity exponent η is obtained from values for $\xi = \eta/\omega$ shown in Table I, based from data on $d \ln \bar{G}_{DP}/d \ln a$. The temporal evolution of the development index a was previously calibrated against population growth rates. Obtaining these estimates and probability distributions for them requires accounting for well-known periodic variations in economic growth rates, as described in the Appendix. Since the estimation formula is nearly linear in ξ , the marginal probability distributions for ξ averaged over the amplitudes of the periodic corrections are to an adequate approximation student t-distributions with a known number of degrees of freedom. For the other cases where an integer is listed in the third column in Table I, this is also the number of degrees of freedom for a student-t distribution. In all of these cases, the number of degrees of freedom is large enough that the distribution is approximately normal except in its tails beyond the ninety-five percent central confidence region.

For each case listed in Table I, the uncertainty in the indicated parameter influences the overall result through its effect on the expansion parameter δ . In each case, the product of δ and the fractional uncertainty listed in the column labeled “ $\Delta V/V$ ” is taken to be small enough to be neglected, so only the maximum likelihood estimates of these parameters are used. The method for estimating “ $\Delta V/V$ ” in each case is given in the Appendix.

The top part of Table II lists estimates of the remaining econometric parameters in the above formulas. The bottom part of Table II lists a number of values derived from these parameter estimates. For the tropical region, the de-

velopment timescale $1/\bar{\nu}$ is about equal to the average difference in age between mothers and children at the time of children’s birth, i.e. one human generation. For the temperate region the development time is slightly lower. Figures 1–3 show the resulting data fits. The values listed for the dimensionless carbon depletion rates $\epsilon_5 = \bar{w}\bar{t}\bar{m}_5$ are for current magnitudes of the slopes \bar{m}_5 for change in carbon intensity vs. cumulative fossil carbon use, which are the only ones directly impacting extrapolations (c.f. Appendix).

TABLE II

Regional parameters

<i>Calibrated:</i>		
Tropical	Temperate	Meaning
2001.6	1966.8	inflection time \bar{t}_0 (Julian yr)
0.0407	0.0517	development rate $\bar{\nu}$ (1/yr)
0.0183	0.0204	intercept f_5 (GT/EJ)
0.0291	0.0122	$1000 \times$ (slope $-\bar{m}_5$ in 1/EJ)
2.0000	2.0000	h =fossil/nonfossil productivity
1.7971	1.4442	$\psi = d \ln E / d \ln a$
5.0964	7.0775	\bar{E} scale (GT/yr)
<i>Derived:</i>		
Tropical	Temperate	Meaning
24.585	19.353	development time $1/\bar{\nu}$ (yr)
0.0013	0.0005	$\epsilon_5 = \bar{w}\bar{t}\bar{m}_5 \ll 1 \Rightarrow$ slow depletion
0.3155	0.4008	development rate $\nu = \bar{\nu}\bar{t}$
0.1791	0.5275	capitalization lag $\delta = \nu\theta\xi$
0.0610	0.0985	$\gamma_2(\delta/2)^2 \sim$ omitted lag correction

Also listed in the bottom portion of Table II are estimates of the ratio ν of the capitalization and development timescales and of the capitalization lag δ . While the estimated capitalization lag is not particularly small for the temperate region, the omitted next order term in the above capitalization factor is proportional to $az\delta^2$, where the product az takes on the maximum value of $(1/2)^2$ at the unit logistic function inflection point where $z = 1 - a = 1/2$. The constants γ_2 , whose values can be computed from the entries for δ in this table, are coefficients in this expansion (c.f. Rethinaraj, 2005). This second order term can readily be included, but this noticeably increases computation times, and adding higher order corrections is at best of marginal use because the expansion in δ is only asymptotically convergent. More accurate solutions can be obtained by numerical integration (Zhang, 2000). However, the estimated accuracy of about ten percent obtained for the global model parameters is adequate for demonstrating the overall features of the growth of extrapolation uncertainties over time, particularly since as shown below the choice of param-

eters characterizing the development function has only a small impact on the overall uncertainty in global average temperatures.

As discussed in detail below, Figures 1, 4, and 5 respectively compare the calibrated theory to data for the evolution of population growth rate, carbon intensity, and fossil carbon use rates. For population growth and carbon consumption, using only the formulas above with annual data leaves clearly statistically significant temporal correlations amongst the residual differences between the data and fits. These must be accounted for before appropriate probability distributions for the theory parameters can be derived from the data. This is done as follows. First, a discrete frequency power spectrum is obtained for the residuals between the theory and the data obtained using the formulas given above. Then the amplitudes of the sine and cosine components of the periodic correction for the largest amplitude periodic mode are estimated. The residuals from the resulting fit are again used to compute a frequency power spectrum and the procedure is repeated until no significant periodicities remain. The statistical test used for this is described in the Appendix. It avoids a situation where it is known to be more likely than not that there remains a statistically significant periodicity in the residuals.

Various additional steps taken here for computational convenience also help avoid a situation where there are known to be statistically significant non-periodic nearest neighbor correlations between temporally adjacent residuals difference of theoretical fits and data: In the case of population and per capita GDP, logarithmic differences are taken to eliminate the need for determining an additional dimensional scale parameter in the fits. This has the additional effect of reducing otherwise expected nearest neighbor correlations. Fitting to logarithms of data was also favored on the grounds that it should reduce a (heteroskadtistic) trend for the residuals between data and model results to become larger when the absolute values of the data increase considerably with time. In the case of carbon intensity, data points are averaged in groups of at least two as described in the Appendix, in order to achieve a uniform spacing in cumulative carbon use as the independent variable. This not only allows for simple application of the discrete Fourier series power spectrum test referred to in the previous paragraph, but also tends to reduce nearest neighbor correlations in residuals between fits and data so averaged. In the case of the more computationally demanding models of the evolution of fossil carbon emissions and the atmospheric heat balances described below, the total number of data points available for use is divided by two through biennial averaging (or by three by triennial averaging for the atmospheric carbon balance). Not only does this usefully reduce the computational burden, it also reduces the tendency of the residuals to exhibit nearest neighbor correlation.

The solid curves in Figure 1 show the periodicity-corrected fits to growth rates of the population increment over its 1820 base value for the tropical and temperate regions. This increment is the population referred to above in the discussion of “development.” The year 1820 chosen for the base year for this calculation is the first year for which annual population estimates are available from the primary data source used (Maddison, 2001 and 2003). This year also

marks the first decade of the “Concert of Europe” which saw the beginning of a long period of strong population growth. Before the Napoleonic Wars that preceded the Concert of Europe and the ultimate global reach of colonialism, population levels and economic production evolved at a much more modest pace.

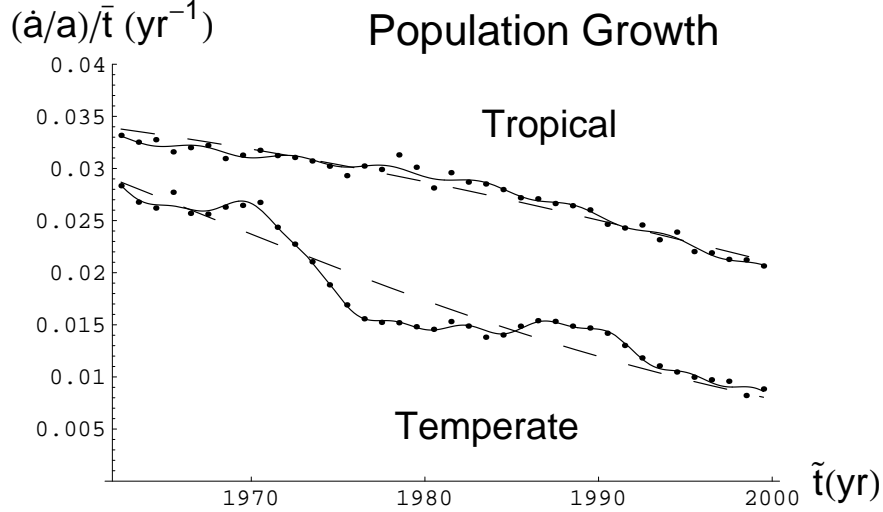


Figure 1. Growth rate $d \ln[\tilde{P} - \bar{P}_{\text{base}}]/d\tilde{t} = \bar{\nu}z + \sum_{n=1}^m \bar{A}_n \sin [2\pi (\tilde{t} - \bar{\tau}_n)/\bar{T}_n]$ $= (\dot{a}/a)/\bar{t}$ of population less preindustrial values, with $a = 1/(1 + \exp[-\bar{\nu}(\tilde{t} - \bar{t}_0)])$ and $z = 1 - a$. The tropical region’s constants are $\bar{P}_{\text{base}} = 0.37$ billion, $\bar{\nu} = 0.0517 \text{ yr}^{-1}$, $\bar{t}_0 = 1996.8 \text{ yr}$, $m=2$, $100\{\bar{A}_n\} = \{0.087, 0.031\}$, $\{\bar{\tau}_n\} - 2000 = \{-6.90, -1.80\} \text{ yr}$ and $\{\bar{T}_n\} = \{38, 38/7\} \text{ yr}$. The temperate region has $\bar{P}_{\text{base}} = 0.68$ billion, $\bar{\nu} = 0.0407 \text{ yr}^{-1}$, $\bar{t}_0 - 2000 = -6.90 \text{ yr}$, $m = 5$, and the periodic corrections parameters are $100\{\bar{A}_n\} = \{0.186, 0.139, 0.078, 0.068, 0.36\}$, $\{\bar{\tau}_n\} = \{3.02, 5.54, 1.32, -0.37, 0.35\} \text{ yr}$, and $\{\bar{T}_n\} = \{38/2, 38, 38/4, 38/2, 38/9\} \text{ yr}$. Dashed curves omit the periodic corrections.

The periods and amplitudes of the periodic corrections for the development index are given in the legend to Figure 1, and for other fits in Table III. The dashed curves in Figure 1 show the “secular” model results for the same logistic function parameters listed in Table I. (The term “secular” refers to a model without periodic corrections.)

Figure 2 compares the secular logistic functions, which are fitted approximations to the ratios of the population increments to their long-term limit values. The denominators in these ratios are the differences between the initial and final population numbers listed on the figures. The long-term limit populations are obtained by minimizing the mean square difference between the population increment data and theory. In can be seen from Figure 2 that the development of the tropical region shows a comparable temporal evolution to that of the

more developed temperate region, trailing behind by the nearly thirty-five year difference in time between the inflection point dates listed in Table I.

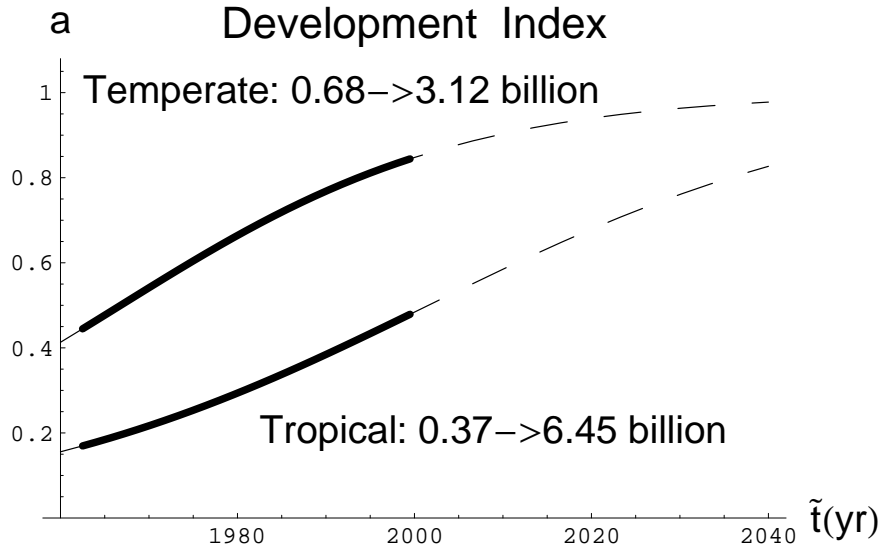


Figure 2. Extrapolated development indices $a = (\tilde{P} - \bar{P}_{\text{base}})/(\bar{P}_{\infty} - \bar{P}_{\text{base}})$, with the constants shown with the notation $\bar{P}_{\text{base}} \rightarrow \bar{P}_{\infty}$. Solid portions of the curves indicate the time range of the data stream used for calibration.

In effect the approach taken here assumes the continued existence of 1820-level subsistence populations relying on traditional energy sources not otherwise accounted for here (like wood and dung) and stuck in a “poverty trap” that allows them too little access to primary energy sources or contribution to regional GDP to substantially affect the rest of the analysis. There is as yet little empirical evidence that this situation is changing, and modeling the probability that sufficient effective international development assistance will be mobilized to substantially change this state of affairs is beyond the scope of the present analysis. For the present purpose, the approach taken here is convenient because it allows for connection to an early period of exponential “balanced growth” of primary energy and GDP increment over the pre-industrial base, without requiring that the total GDP extrapolate back essentially to zero in the base year 1820 on the development timescales listed in Table I.

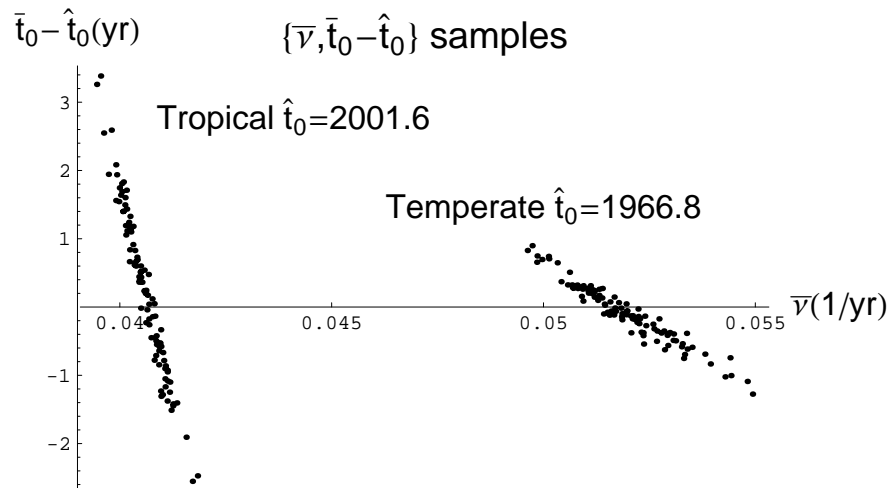


Figure 3. Scatter plots of 100 random samples of initial development rate, with the indicated maximum likelihood estimates \hat{t}_0 subtracted from inflection time samples \bar{t}_0 so that both regions can be plotted on the same graph.

Scatter plots for a hundred random samples each of the development index parameters $\{\bar{v}, \bar{t}_0\}$ are given for the tropical and temperate regions in Figure 3. To allow these to be plotted on the same graph, the maximum likelihood estimates \hat{t}_0 indicated on this figure for each region have been subtracted from the inflection time \bar{t}_0 samples before plotting. The method used for obtaining these plots was rejection sampling. Details on this sampling method are described in the Appendix.

The data range used to compute the results shown in Figures 1 and 2 covered the years 1962–2000 inclusive. Since the population data are differenced to obtain growth rates, temporal averaging is inconvenient, and is also unnecessary and avoided in this case. The starting date of 1962 is chosen primarily to avoid the period of rapid re-capitalization that occurred during the first two capitalization times after World War II when fitting per capita GDP over the same time range. As shown by Barro and Sala-i-Martin (1995, Section 10.2), after WWII the major combatants underwent an economic readjustment on about this capitalization timescale that returned them to near their historical rates of growth of per-capita GDP. The choice of 1962 for a starting date also just avoids the period of the Chinese “Great Leap,” which produced a population deficit of about thirty million people compared to the pre-existing trend. To include the center of the Great Leap period in the population database would introduce a clear outlier and require a modification of the mathematical methods used. For these reasons we postpone the econometric modeling of such turbulent times to future studies. No other clear outliers in the differences between data

and maximum likelihood fits were observed during inspection of all residuals from fits done for this paper.

It is both convenient and sufficient to use in the succeeding calculations only the secular approximations for the development index, sampled from the bivariate marginal probability distribution obtained by integrating over other parameters in the probability distributions as described in the Appendix. This is convenient because it enormously simplifies the solution for utility maximization for the succeeding portions of the model. It is sufficient because empirical periodic corrections to the desired fossil carbon use rates are in any case included in the fits of the theory for the succeeding portions of the model. The underlying theoretical assumption is that the economies respond to the average background trends in growth of population and development, with periodicities in actual carbon use reflecting business and energy pricing cycles superimposed on the resulting background trends.

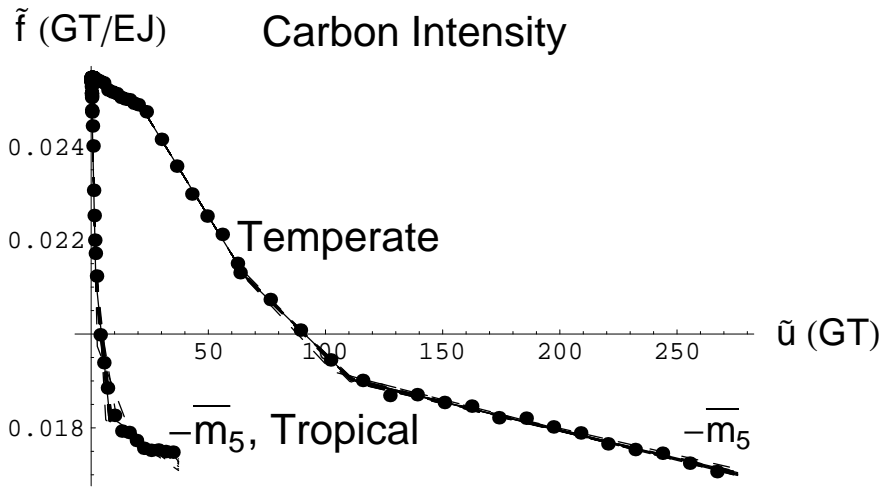


Figure 4. Piecewise linear maximum likelihood fits (solid lines) and sets of twenty random samples (dashed lines) for the line segments' slopes and intercepts, for carbon intensity of energy production as a function of cumulative carbon use. The portion of the fits labeled “ $-\bar{m}_5$ ” have slope $-\bar{m}_5$ and are extrapolated as a linear function of cumulative carbon use until a change of slope is chosen as exemplified in Figure 8.

Fits to data on the carbon intensity of energy use are shown in Figure 4. The piecewise linear and bold dashed lines in Figure 4 include the line defined by the intercept and slope listed in Table II. Also shown in Figure 4 are results from twenty random samples for the slope $-\bar{m}_5$ and intercept \bar{f}_5 for these segments, and for the preceding line segment. Since the fitting functions are linear in all of the fitting parameters, under the assumption that the residual differ-

ences between the data and the fits are independently and identically normally distributed (normal iid), the marginal probability distributions for the pairs of slopes and intercepts for these lines have a bivariate student t-distribution (Box and Tiao, 1972, p. 45).

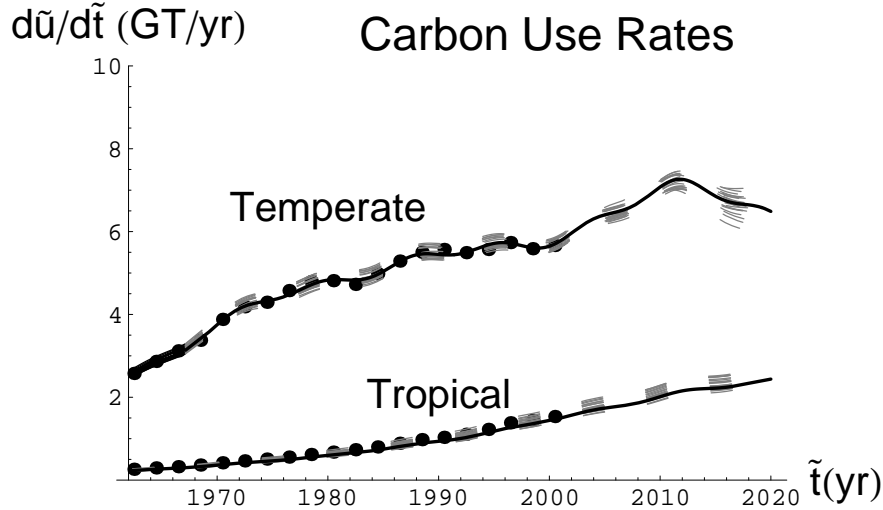


Figure 5. Carbon use rate fits vs. biennially averaged data for maximum likelihood estimates (solid curves) and sets of twenty random samples (dashed curves). The solid curves multiply results using the secular parameters in Table II by corrections of the form $\exp[\sum_{n=1}^3 \bar{A}_n \sin[2\pi(\tilde{t} - \bar{\tau}_n)/\bar{T}_n]]$ where the periods \bar{T}_n , phases $\bar{\tau}_n$, and amplitudes \bar{A}_n for solid curves are listed, from the rightmost column for $n = 1$ to the leftmost column for $n = 3$, in the upper part of Table III. The parameters sampled using the methods described in the Appendix are the scale \bar{E} , development index exponent ψ , the amplitudes of the sine and cosine contributions to the periodic corrections, and the frequency of the periodic correction that has the longest period. Fits are done to logarithms of carbon use rates, so to a good approximation it is the sum of squares of the fractional rather than absolute differences between data and the maximum likelihood fitting function that is minimized to produce the solid curves.

Results for calibration, sampling, and near-term extrapolation of fossil carbon use rates for the tropical and temperate regions are shown in Figure 5. The dark solid curves are maximum likelihood fits, and the lighter dashed curves result from taking twenty random samples of the fitting parameters. To produce these results, it is necessary to solve the fossil carbon balance equation, which in dimensional variables can be written in the form

$$\bar{v}zad\tilde{u}/da = \bar{w}\tilde{f}_k(1 + bh\tilde{f}_k/\bar{f}_1)a^\psi F^{\alpha/\omega}$$

with $\tilde{f}_k = \bar{f}_k - \bar{m}_k \tilde{u}$ and $b = (h - 1)/h$. Here \bar{v} is the initial population and development growth rate for each region in 1/yr, \tilde{u} is its cumulative carbon use in Gtonne, $\bar{w} = \bar{E}/\bar{f}_1$ is its long-term limit energy use rate in EJ/yr, and \tilde{f}_k for $k = 4, 5$ are the carbon intensities of energy use respectively for the earlier and later downward sloping line segments shown in Figure 4. The normalization constant $\bar{f}_1 = 0.0255$ GT/EJ is the nominal intensity for earliest times when only coal was used as a primary energy source as operationally defined here. The left hand side of the above fossil carbon balance equation results from the property of the unit logistic function a that $d/d\tilde{t} = \bar{v}zad/da$ with $z = 1 - a$. The right hand side accounts for the assumption that the energy production efficiency for a given level of development decreases in the limit of maximum cumulative carbon use by a factor of h . This results because $b = (h - 1)/h$, and $p = (1 + bh\tilde{f}_k/\bar{f}_1)$ takes on the value h at the beginning when $\tilde{f}_1 = \bar{f}_1$ and the value 1 in the energy sustainability limit where $\tilde{f}_7 \rightarrow 0$.

TABLE III

Periods, phases, and amplitudes for periodic oscillations

<i>Tropical Emissions:</i>			
Period (yr)	40.13	13.00	7.80
Phase (yr from 2000)	-2.72	2.93	1.92
Amplitude (%)	2.52	0.72	1.52
<i>Temperate Emissions:</i>			
Period (yr)	36.04	19.50	7.80
Phase (yr from 2000)	6.64	-3.41	1.70
Amplitude (%)	6.65	3.68	1.77
<i>Global Temperature:</i>			
Period (yr)	64.23	20.64	
Phase (yr from 2000)	5.90	-2.13	
Amplitude (°C)	0.101	0.044	

The fossil carbon balance equation can be analytically integrated to give

$$\ln\left[\frac{(bh\bar{f}_k/\bar{f}_1) + 1/(1 - \tilde{u}\bar{m}_k/\bar{f}_k)}{(bh\bar{f}_k/\bar{f}_1) + 1/(1 - \bar{u}_4\bar{m}_k/\bar{f}_k)}\right] = \epsilon_k(S[a] - S[a_4])$$

where $S[a] = \int_0^a da a^\psi (1 + a\delta)^{\alpha/\omega} / (za)$. Here the last historically determined development index break point a_4 for each region and the cumulative carbon use \bar{u}_4 at this break point are known from the carbon intensity fitting procedure. This analytically integrated fossil carbon balance equation is readily solved for \tilde{u} . The result is inserted into the above expressions for carbon intensity \tilde{f}_k and the production efficiency factor p . This allows evaluation of the carbon use rates $\bar{E}(\tilde{f}_k/\bar{f}_1)(1 + bh\tilde{f}_k/\bar{f}_1)a^\psi F^{\alpha/\omega}$. The Appendix shows how the integral $S[a]$ can be expressed in terms of a hypergeometric function.

Given the known existence of short-term business cycles and longer periods of energy cartel efficacy and inefficacy, it is to be expected that periodic corrections will be needed to the underlying trends in fossil carbon use obtained from the above formulas. The method for estimating these corrections follows that described above for population and GDP growth rates, with one exception. This exception is that the frequency of the longest period is taken as a fitting parameter. In the cases described above it was sufficient to fix this frequency to correspond to the longest period that was statistically significant in the discrete Fourier power spectrum of the residuals between the secular model and the data. This was all that was needed to make the final residuals apparently iid, and since only the parameters describing the secular parts of the model were subsequently needed it was not necessary to obtain an accurate sampling of the periodic behavior. In the case of the rate of fossil carbon use, however, it is both tractable to numerically integrate the effect of periodic variations on the atmospheric carbon and heat balances and interesting to track the non-secular variations of carbon use at least into the near future. However, fixing the frequency of the fairly large amplitude longest period oscillations would overestimate the accuracy with which the phasing of these oscillations can be traced into the more distant future. To avoid this difficulty, it is necessary to sample the frequency of the longest period oscillations, as described in the Appendix.

In the fits and extrapolations shown in Figure 5, the leveling off of the fossil carbon use rate around 1980 and in the 1990s correspond respectively to the first oil cartel period and to reform of centrally planned economies in the temperate region (which includes China as well as the former Soviet block). If the roughly linear growth in carbon use rate observed on the average for the temperate region from 1974–96, resumes, then the increasing pressure on the oil portion of this carbon use would be expected to stimulate energy substitution and conservation measures. This would lead to downward pressure on carbon use unless oil is replaced primarily by coal, which is possible but difficult given the current predominant use of oil as a source of transportation fuel. Just how large such a correction would be is highly uncertain. According to the present broad-brush empirical treatment of such oscillations, for the twenty random samples shown the result by 2015 for the temperate region could range anywhere from little reduction below peak levels of carbon use rate to a return nearly back down to late twentieth century levels. Carbon use by the tropical region (which notably includes India), on the other hand extrapolates to be appreciably greater in 2015 than in 2000 in all twenty tropical region samples. The exact timing and extent of a post-2015 temperate region carbon use rate downturn may depend on the details of the fallout from the 2003 invasion of Iraq. That event followed the renaissance of effective oil cartel pricing at the end of the twentieth century slightly more rapidly than the Iran-Iraq War followed the onset of first effective oil cartel pricing in 1973. The details of how all of this occurs lie well beyond the scope of the present model. The main point here is that, from a statistical analysis point of view, accounting for the existence of non-secular variations can be significant when fitting and sampling models

based on data that include the kind of variations that occurred in the latter part of the twentieth century.

The scale \bar{E} of the long-time-limit carbon use rates listed in Table II of about five Gtonne per year for the tropical region is less than that of seven Gtonne per year for the temperate region, despite the more than two-fold larger long-term limit population in the tropical region. This might at first glance seem surprising, since a wide range of carbon emissions scenarios from the Intergovernmental Panel on Climate Change have higher carbon emissions evolving in developing than developed regions (e.g. in Nakicenovic, 2000). However, on closer examination the reasons for this become apparent:

First, because of its low population growth rate over the data calibration period used, China is included in the temperate region here. China is instead lumped with developing countries in many other studies.

Second, it is common in scenario building to extrapolate a growth rate for developing countries' GDP that is higher than for developed countries. This has the inevitable result that the total GDP for the developing countries eventually becomes higher than for the developed ones if the extrapolation is taken out far enough. The use in the present work of a logistic function raised to a power for the extrapolation of economic productivity allows the data calibration to determine whether extrapolated GDP for a region with current higher growth rate eventually overtakes a more developed region that currently has lower growth rate. If the less developed region is still deep in its exponential growth phase then it will overtake the more developed one. However, in the present case the tropical region has the maximum likelihood value for the inflection point time for its productivity coefficient a^ψ in the year 2016 and passes out of its exponential growth phase during the 1960–2020 time range plotted above in Figure 5. Of course if there is a break in the historical pattern, for example through a significant shift to effective foreign aid to break the poverty cycle in Africa (c.f. Sachs, 2005), then the range of extrapolations based on the present model could be exceeded. It would be interesting to estimate the probability of such an enterprise on effective poverty alleviation being attempted and succeeding, but incorporating such estimates is beyond the scope of the present paper.

A third reason for moderation of carbon use rates in the tropical region is that the linear growth phase around its inflection point is occurring at a time when the decrease in carbon intensity of energy production, f , and its effect through $p = 1 + (h - 1)f$ on energy productivity is more pronounced than was the case in 1974 when the temporal region passed through the inflection point of its productivity coefficient a^ψ . In part for the reasons just listed, it will not be surprising to see below that the overall fossil carbon emissions rates shown below in Figure 9 are comparable to the lower emissions rate scenarios reported in scenario B1 from the IPCC Third Assessment Report than for several other scenarios in that report (IPCC, 2001) .

3. Atmospheric Response

The equations used to model the fractional increase c and increase \tilde{T} respectively of atmospheric carbon loading and global average temperature over their pre-industrial base values are (Petchsel-Held et al., 1999):

$$\begin{aligned}\tilde{C}_0 dc/d\tilde{t} &= \bar{B}\tilde{F}_{\text{net}} + \bar{\beta}\tilde{E}_{\text{net}} - \bar{\sigma}\tilde{C}_0 c \\ d\tilde{T}/d\tilde{t} &= \bar{\mu} \ln[1 + c] - \bar{\alpha}\tilde{T}\end{aligned}$$

Here $c = (\tilde{C} - \tilde{C}_0)/\tilde{C}_0$ where \tilde{C} is the atmospheric carbon dioxide concentration. The pre-industrial atmospheric carbon dioxide concentration from the data we use is $277.0 \pm 0.1 \approx 277$ parts per million (ppm by mass) for 1700–1755, so the preindustrial atmospheric CO_2 concentration is taken to be given at $\tilde{C}_0 = 277$ ppm (Rethinaraj, 2005). \tilde{E}_{net} is η_{net} times the total global fossil carbon use rate, and \tilde{F}_{net} is the cumulative value of \tilde{E}_{net} . One could set $\eta_{\text{net}} < 1$ to account for incomplete combustion, but we also omit gas flaring and bunker fuels used in air and sea transport (which are not readily assigned to a particular region’s consumption) and CO_2 emissions from production of cement (for which we have not assembled a comparably complete and disaggregated database). These omissions are all small and approximately compensate each other, so for simplicity here we set $\eta_{\text{net}} = 1$. We also neglect the effect of secular changes in land use on carbon emissions. These changes may dominate nineteenth century net carbon emissions and still be comparable to the effects of fossil carbon use in the early twentieth century, which is one of the motivations for using only the Mauna Loa data from the second half of the twentieth century for calibrating the atmospheric carbon balance model (Keelling and Whorf, 2005). Whether there is any significant net effect of land use changes on cumulative carbon emissions by the end of the twentieth century is not completely clear (Jain and Yang, 2005), so for simplicity we also neglect their impact on \tilde{F}_{net} .

For the preindustrial global average temperature, data that is comparably stable and accurate as that for atmospheric CO_2 are not available. Thus the base level temperature is taken to be a fitting parameter. Only the increase over this value is reported for modeling results for \tilde{T} . For the maximum likelihood reference model results here, the fitted value for the preindustrial base level is 0.004 ($^{\circ}\text{C}$) lower than the low point of the biennially averaged global average temperatures data from 1857–2000, which is found at 1907–08. Thus for this case the 1907–08 average, which is unusually low for the twentieth century, is almost exactly equal to the inferred preindustrial base value.

The constant $\bar{\beta} = 0.47$ in the above equations converts Gtonne elemental carbon to ppm atmospheric CO_2 . The long-term limit \bar{F}_{net} of cumulative carbon emission in this model effects a long-term increase in atmospheric carbon content and global average temperature through saturation of near-surface carbon reservoirs. The net long-term effect on atmospheric carbon loading increase proportional to the constant $B = \bar{B}/(\bar{\beta}\bar{\sigma})$.

The constant $\bar{\mu}$ is a measure of the greenhouse effect. At the rough approximation level used here, only the greenhouse effect of fossil carbon emissions is

taken to be secular. All other greenhouse effects are implicitly subsumed in the periodic corrections that are required to make the residuals between the data and global average temperature data apparently iid according to the statistical tests used.

The very simple model used here for drivers of global average temperature is fortuitously approximately adequate for the historical data period examined, for two reasons. One of these is that the (primarily secular) effect of other anthropogenic radiative forcings approximately cancels out. These include the warming effect of CH_4 , N_2O , well-mixed trace gases, and ozone and the cooling effect of anthropogenic aerosols. A more complete assessment of outcome probabilities would include detailed models of the past and future of each of these effects, rather than approximate their slight net historical warming effect as exact cancellation and implicitly assume that such cancellation will continue in the future.

Another simplification follows from the observation that the effects of changes in solar irradiance and stratospheric aerosols in sum are both primarily non-anthropogenic and non-secular. Shorter period changes in solar irradiance connected with sunspot cycles are known to be intrinsically periodic, and any significant longer term changes on century time scales may be as well. The stratospheric aerosol effect is driven primarily by volcanos and is perchance approximately periodic over the time of availability of direct atmospheric temperature measurements. This is due to comparable periods of enhanced volcanic activity starting with Krakatoa in 1883 and Agung in 1963. A more complete treatment of such non-secular influences on global average temperature would explicitly account for changes in solar irradiance and rely on observations of individual past volcanic eruptions and a stochastic model of future production of stratospheric aerosols. For an extensive recent discussion of these issues pertinent to the simplifications used here, see Hansen et al. (2006).

TABLE IV

Atmospheric carbon balance and heat balance parameters

<i>Carbon:</i>	
Value	Meaning
0.0449	CO ₂ relaxation coefficient $\bar{\sigma}$ (1/yr)
0.2296	saturation coefficient $B = \bar{B}/(\beta\bar{\sigma})$
0.1411	c , 1960 fit ($\Rightarrow \bar{C} = 316$ ppm in 1960)
<i>Heat:</i>	
Value	Meaning
0.0171	thermal relaxation coefficient $\bar{\alpha}$
0.0170	$\bar{\alpha}$ prior mode in yr ⁻¹
0.0979	opacity effect coefficient $\bar{\mu}$ (°C)/yr
-0.0040	lowest data is preindustrial plus $\bar{T}_0 = -0.0040^\circ\text{C}$

The atmospheric carbon loading and global average temperature changes in the approximation used here respectively respond immediately to carbon emissions and increases in atmospheric carbon content. Thus, for example, the greenhouse effect coefficient $\bar{\mu}$ is heavily constrained by the data. However physical climate models suggest that the temperature relaxation coefficient $\bar{\alpha}$ is so small that it is not well conditioned by the data used for calibration in the present study. It was thus found desirable to apply a prior probability distributions for $\bar{\alpha}$. Since on physical grounds $\bar{\alpha} > 0$, we use a log-normal prior probability distribution for it. The extraction of such distributions from physical principles without “double counting” the data subsequently used for model calibration involves subtleties that are avoided here simply by adopting log-normal prior probability distributions with modes determined by a literature reference value. The prior mode for $\bar{\alpha}$ from Petschel-Held et al. (1999) is listed in Table IV. Also listed in Table IV are the maximum likelihood values for all of the atmospheric response parameters, given the data used, for a standard deviation in the log-normal prior for $\bar{\alpha}$ of 0.3. Sampling results for these prior standard deviations set to 0.2 and 0.4 were also obtained, as described below.

TABLE V

Influence of prior on carbon balance parameter estimates

prior σ_B	0.20	0.30	0.40	∞
$B = \bar{B}/(\bar{\beta}\bar{\sigma})$	0.2166	0.2192	0.2209	0.2296
$\bar{\sigma}$	0.0435	0.0438	0.0440	0.0449
$c = (\bar{C} - \bar{C}_0)/\bar{C}_0$ in 1960	0.1407	0.1408	0.1408	0.1411

The value of the dimensionless constant $B = \bar{B}/(\bar{\beta}\bar{\sigma})$ is important for the present study, since in the long-term sustainable ($\tilde{E}_{\text{net}} \rightarrow 0$) limit, the post-industrial increase in atmospheric carbon dioxide concentration levels off at a value proportional to cumulative carbon emissions as $\bar{C}_0 c \rightarrow B\bar{\beta}\bar{F}_{\text{net}}$. The value of $\hat{B} \approx 0.23$ for B listed in Table IV is twice the mean of the range 0.08–0.15 from “dissolution chemistry of carbon in the oceans” quoted by Petschel-Held et al. (1999) from Maier-Reimer and Hasselmann (1987). As shown in Table V, the data used here demands this result even if a very informative prior probability distribution for B is included when computing a maximum likelihood estimate. In particular, very nearly the same estimate for B is obtained after imposing a log-normal prior probability distribution for B with a standard deviation as small $\sigma_B = 0.2$. The value $\sigma_B = 0.2$, corresponds to a ninety-five percent prior confidence range of only 0.08–0.16. Given these results, for the fits and extrapolations shown here we decided to therefore sample the posterior probability distribution without using any informative prior for B .

Fits to the fractional increase c in atmospheric carbon dioxide concentration over the preindustrial base are shown for twenty random samples in Figure 6. This figure shows the range of self-consistent data on triennially averaged atmospheric carbon dioxide measurements from 1959–2000 used to calibrate the atmospheric carbon balance model. For these fits there is no need for periodic corrections if the data are averaged in groups of three adjacent years, which considerably simplifies the analysis. (With less data averaging periodic corrections are required according to the statistical test used here, but their amplitudes are very small.)

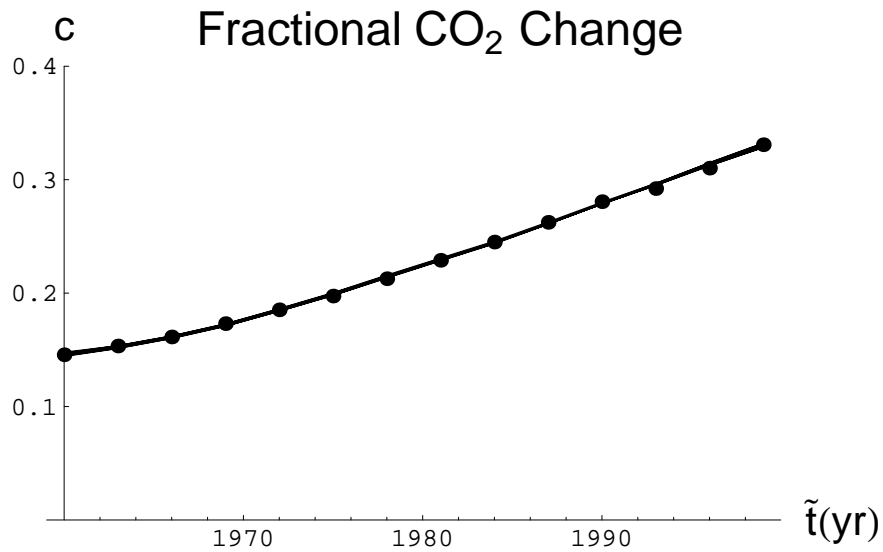


Figure 6. Fractional change $c = (\tilde{C} - \tilde{C}_0) / \tilde{C}_0$ of atmospheric CO₂ concentration plotted for triennially averaged data and twenty random samples. $(\tilde{C} - \tilde{C}_0)$ is the increment of CO₂ over its pre-industrial base value of $\tilde{C}_0 = 277$ ppm.

For global average temperature, the discrete Fourier power spectrum of the residuals between data and the secular model reveals two statistically significant periodicities. Both of these are readily apparent in the twenty random samples shown in Figure 7. For convenience, the zero level in Figure 7 is taken to be the 1907–1908 average temperature, so what is plotted there is $\Delta\tilde{T} = \tilde{T} + \tilde{T}_0$, where $\tilde{T}_0 = -0.004^\circ C$. Given the size of the amplitudes of the periodic corrections, the frequencies of both are varied for maximum likelihood fitting and subsequently sampled. This is done to avoid overestimating the accuracy with which the phase of either of these variations can be projected into the future and thus produce spurious oscillations in the spreads of global average temperature described below.

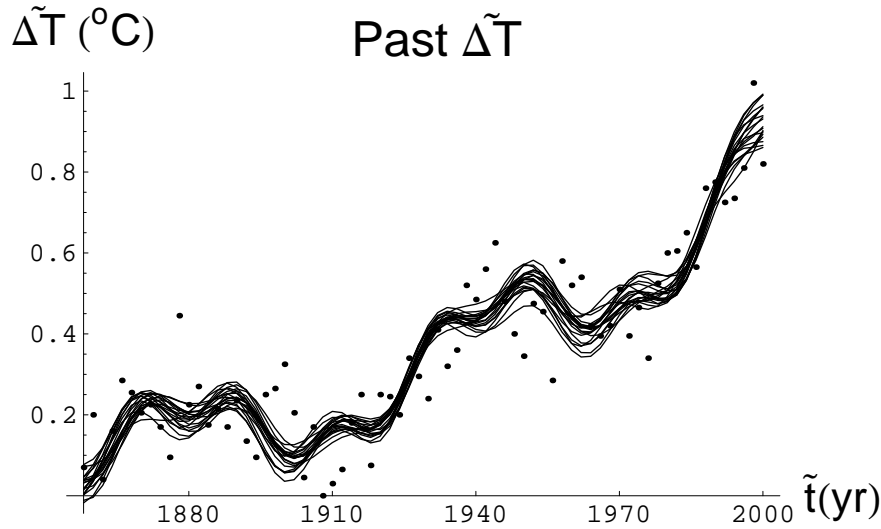


Figure 7. Temperature increment over the lowest of the biennially averaged global average temperatures for twenty random samples.

4. Projection Uncertainties

With the random samples of fitting parameters described above, it is possible to construct random samples of future carbon use, the atmospheric carbon balance, and global average temperature that are appropriate as long as the formulas used are applicable. However, caution in pushing this too far is suggested by the historically observed breaks in slope of piecewise linear fits to the carbon intensity as a function of cumulative carbon use. To account for uncertainties about expected future changes in the slope of this relationship, as outlined qualitatively in the Introduction section above, we have allowed for and sampled the parameters of two additional future breaks in this slope. In describing this model quantitatively here, carbon intensities are divided by the nominal value for coal. Thus, for example, the carbon intensity for natural gas is $f_{\text{gas}} = 0.54$.

To account for the difficulty of reducing the average carbon intensity of energy use below the value for natural gas, a log-normal distribution with a mode for the next break point at near this carbon intensity is sampled. The result is $f_{\text{break}} = \text{Max}[0, f_{\text{now}} - (f_{\text{now}} - f_{\text{gas}})d_1]$, where d_1 is sampled from a log-normal distribution with standard deviation σ_{prior} . Here f_{now} is the carbon intensity at the last fitting point in the reference model, which for maximum likelihood parameters is coincidentally nearly equal at 0.67 for the temperate region and tropical regions. At this next break point the magnitude of the slope for the temperate region is divided by $(1 + d_2)$ where d_2 is also sampled from a log-normal distribution with standard deviation σ_{prior} . For the sample mode at $d_2 = 1$ this cuts the magnitude of the slope in half.

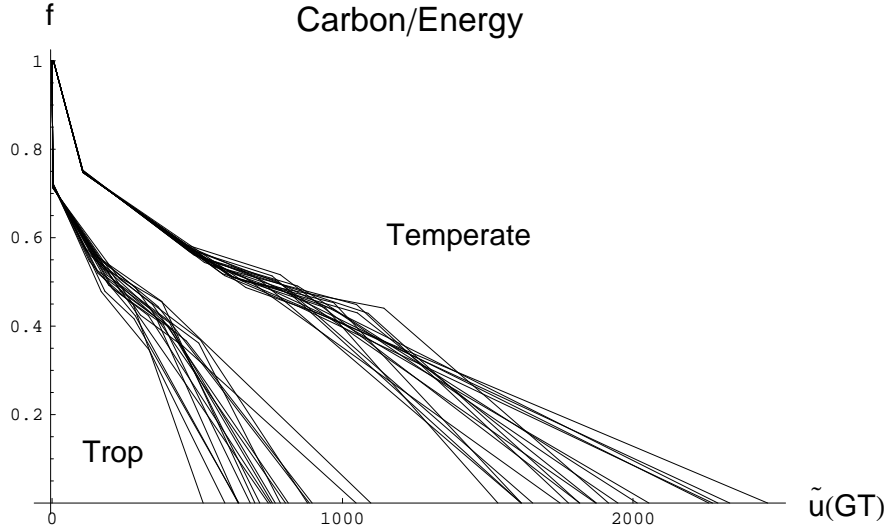


Figure 8. Carbon intensity of energy production for sets of twenty random samples.

The mode values chosen for the next break point, here called f_{act} , are the carbon intensities of energy production when total cumulative fossil carbon use over all previous time is 1200 Gtonne with all maximum likelihood parameters in the model. This occurs in this reference simulation at year 2103, when global average temperature increment over preindustrial values with these parameters is 2.05°C. The resulting values for f_{act} are comparable, at 0.44 for the tropical region and 0.47 for the temperate region. The next break point is at $\text{Max}[0, f_{\text{break}} - (f_{\text{break}} - f_{\text{act}})d_3]$ where d_3 is sampled from a log-normal distribution with standard deviation σ_{prior} . At this point we revert back to the most historically observed slope of carbon intensity vs. cumulative use, times a factor d_4 sampled from a log-normal distribution with standard deviation σ_{prior} . This centers this slope back on the larger historically achieved magnitude, but with a large range of uncertainty assumed here to be appropriate for extrapolations

to such a distant future. The results shown in Figures 8–13 in all cases use a reference value of $\sigma_{\text{prior}} = 0.3$.

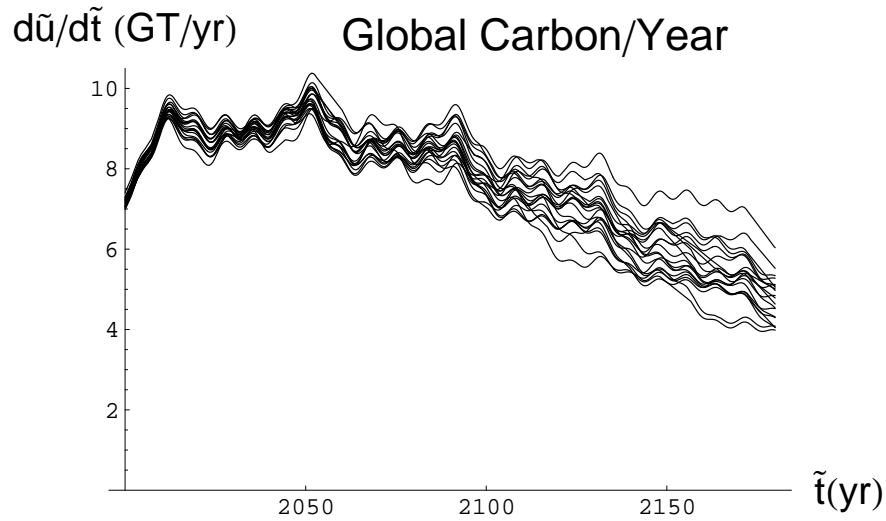


Figure 9. Total global carbon burning for twenty random samples.

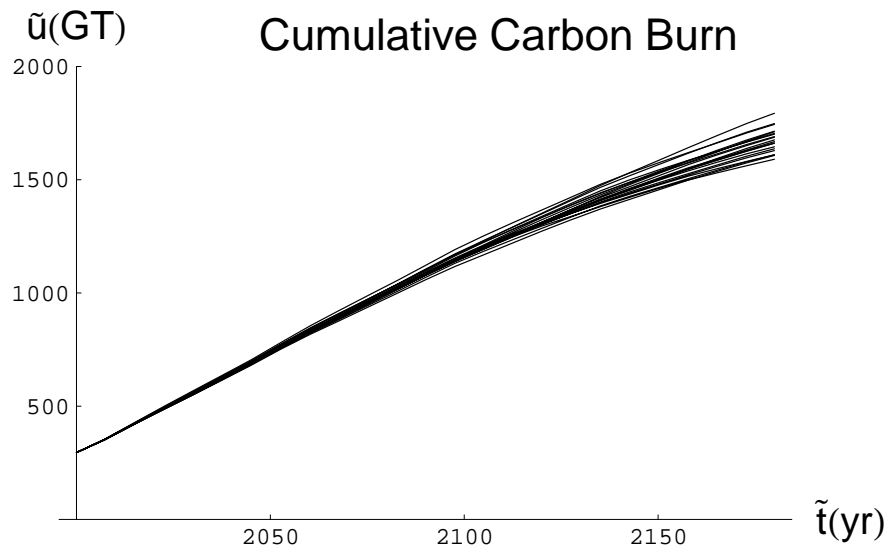


Figure 10. Cumulative carbon burning for twenty random samples.

Projections for twenty random samples of annual and cumulative global carbon burning are shown in Figures 9 and 10 respectively. The early twenty-first century surge in carbon use rate is succeeded by a correction for about three decades down to the 8–9 Gtonne/yr range. After this, an approach to saturation

in total primary energy use rate combines with the decline of carbon intensity illustrated in Figure 8 to produce a long declining trend in carbon emissions. As would be expected from any sensible uncertainty analysis, the uncertainty for carbon emission rates for most of the twenty-second century is comparable to their magnitude. The same cannot be said about the uncertainty for cumulative fossil carbon emissions. Given previous history and another half century of annual emissions in the 8–9 Gtonne range, cumulative carbon emissions through the twenty-first century are tightly constrained, and an appreciable fanning of projections for cumulative carbon emissions is only evident in the twenty-second century.

Note that the near stagnation of growth in carbon emissions and its subsequent decline in the second half of the twenty-first century occurs despite the fact that what is conceptually thought of here as a “new age of coal” moderates the recent historical slope of decline of the carbon intensity of energy production as a function of cumulative carbon use. The saturation and gradual decline of carbon emission rates in the twenty-first century follows primarily from modest rates of extrapolated growth resulting from fitting the model used here to historical data. Also, the projections done here have the carbon intensities of energy production divided by that for pure coal on the order of one-half (e.g. natural gas dominated) for most of this century, as opposed to their recent values of about two-thirds. This results only from extrapolating recent historical trends down to the point where the carbon intensity of energy production is on the order of one-half, not from assuming that a global agreement on limiting carbon emissions keeps the recent historical trend continuing without interruption. It is only the steeper rate decline of global carbon emissions rate in the following century that results from a sampling a distribution of this slope centered on the maximum likelihood value of its recent historical average. That such globally effective action to accelerate the trend to asymptotic approach to zero carbon emissions occurs at some point randomly sampled around the carbon intensity that corresponds to enough cumulative global carbon emissions to raise global average temperatures by just above two degrees Celsius above pre-industrial levels is, of course, just one of many hypotheses that could be chosen for such extrapolations. It serves here, however, to provide an example of how such a hypothesis can readily be incorporated into the present approach.

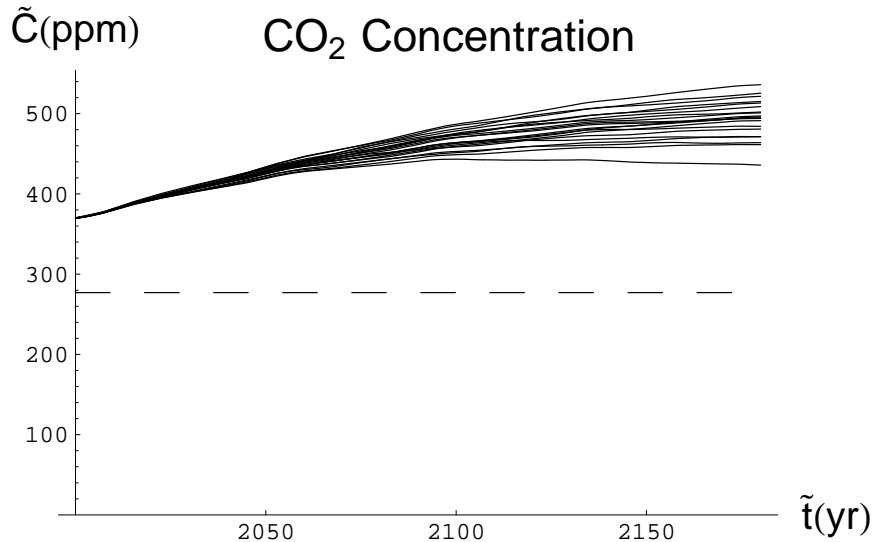


Figure 11. Atmospheric carbon concentration for twenty random samples.

Atmospheric carbon concentrations are heavily influenced by the fairly well defined emissions rate in the first half of the twenty-first century. In the twenty-second century the saturation effect represented by the parameter \bar{B} in the atmospheric carbon balance equation slaves atmospheric carbon concentrations to a fairly sharply defined level of cumulative emissions. As shown in Figure 11, the net result is a fairly narrow spread of projections for atmospheric carbon concentrations. All of this is the context of a very simple linear differential equation whose three-parameter solution set is tightly constrained by the small and apparently random variations of triennial averages of reported data. It has been noted above that the maximum likelihood estimate $\hat{B} \approx 0.23$ of the parameter $\bar{B}/(\beta\bar{\sigma})$ from this procedure differs by a factor of two from that inferred from physiochemically based modeling. Using the maximum likelihood parameters data-calibrated here, this model nevertheless gives lower atmospheric CO₂ concentrations when run to 2100 than the CO₂ levels reported in IPCC Third Assessment Report (IPCC, 2001) as resulting from similar emissions in the B1 scenario. Thus it would not be surprising if the result of small spread in projected global atmospheric carbon concentrations fails to be robust in future work against the systematic sampling of larger parameter sets used to calibrate more complete atmospheric carbon balance models.

Growth of the uncertainty in global average temperatures is illustrated in Figure 12. The coherence in phasing of periodic fluctuations of temperature is evident above in Figure 7 and continues into the first two decades of the twenty-first century. Thereafter coherent phasing amongst the various samples is rapidly lost. To give an idea of the periods and amplitudes of the dominant periodic variations, Table VI lists the maximum likelihood values of the periodic corrections to the secular parts of the atmospheric carbon and heat balance

models. (The numbers under the period listed at the top of each columnar set of figures are the phase and amplitude corresponding to that period.) Through the compounding of uncertainties in atmospheric carbon concentrations with uncertainties in the atmospheric heat balance model parameters, the spread in projected global average temperatures increases appreciably with time.

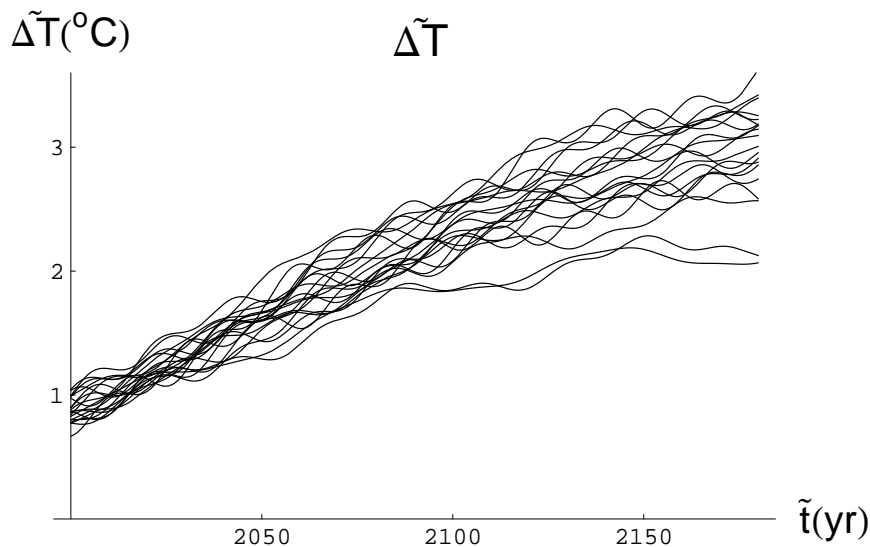


Figure 12. Global average temperature increase for twenty random samples.

TABLE VI

Periods, phases, and amplitudes of periodic corrections

<i>Tropical Emissions:</i>			
Period (yr)	40.13	13.00	7.80
Phase (yr from 2000)	-2.72	2.93	1.92
Amplitude (%)	2.52	0.72	1.52
<i>Temperate Emissions:</i>			
Period (yr)	36.04	19.50	7.80
Phase (yr from 2000)	6.64	-3.41	1.72
Amplitude (%)	6.65	3.68	1.77
<i>Global Temperature:</i>			
Period (yr)	64.23	20.64	
Phase (yr from 2000)	5.90	-2.13	
Amplitude (°C)	0.101	0.044	

While the sets of twenty random samples shown in Figures 9–12 give a qualitative impression of ninety-five percent confidence levels, for a quantitative measure a larger number of samples is needed. Figures 13a–d show cumula-

tive normal distribution fits to the central ninety-five of cumulative distribution centiles produced by sorting samples in ascending order. Except for tails of the distributions that taken together correspond to low probability outcomes, the cumulative normal fits are sufficiently good that the distributions at each point can be simply characterized by a mean and standard deviation.

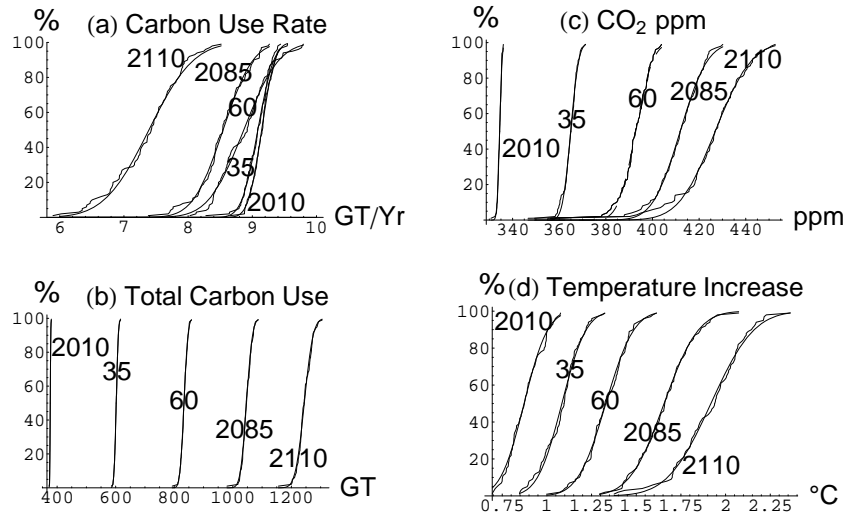


Figure 13. Cumulative probability distribution centiles (jagged plots), and cumulative normal distributions fit to the central ninety-five centiles (smooth curves) for the indicated Julian years for global totals for (a) annual carbon use rate, (b) cumulative carbon use, (c) atmospheric CO₂ concentration, and (d) increase in average temperature due to anthropogenic carbon use. The curves labeled 35 and 60 are for 2035 and 2060 respectively.

The growth of the standard deviation for global average temperature increase can be well fit by a simple quadratic function of the mean projections for global average temperature increase. Such fits taken from quinquennially spaced results like the ones shown in Figure 13d are shown in Figure 14. For the maximum likelihood model a power law fit gives an exponent of 1.84, and a simple quadratic fit is adequate for the present purposes. The results shown in Figure 14 are for three values of the standard deviations σ_{priors} of the above-mentioned prior probability distributions. Essentially indistinguishable from the result for $\sigma_{\text{priors}} = 0.3$ is that for a 1:2:1 binomial distribution values of 0.2, 0.3, and 0.4 for these prior standard deviations. This accounts not only for the prior uncertainty, but in a very rough way also for the uncertainty in that uncertainty. Evidently the specific assumptions about these prior uncertainties are not particularly important for the result shown in Figure 14.

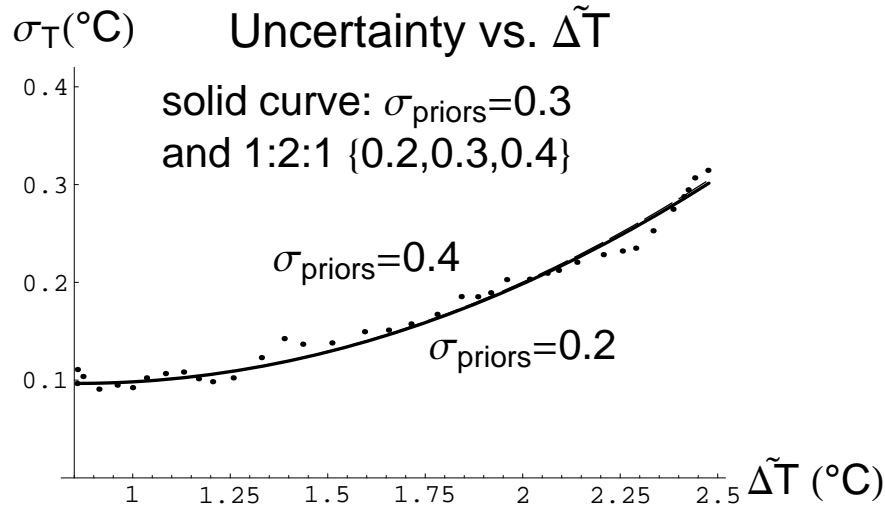


Figure 14. Standard deviation σ_T versus mode for global average temperature increase ΔT for quinquennially spaced fits of the type shown in Figure 13d (dots) and for quadratic fits to increases over year 2000 values. Dashed curves are fits for the indicated standard deviations σ_{priors} for h (the “fossil/non-fossil energy productivity ratio”) and $\bar{\alpha}$, the global average temperature relaxation coefficient. The solid curve, for a 1:2:1 weighting of results for $\sigma_{\text{priors}} = 0.2, 0.3,$ and $0.4,$ is so close to the result for $\sigma_{\text{priors}} = 0.3$ that it overwrites the dashed curve for that reference value of $\sigma_{\text{priors}} = 0.3,$ and also the dashed curve for $\sigma_{\text{priors}} = 0.2$.

To provide some insight into the sources of projection uncertainty, Table VII shows the percentage decrease in the standard deviations of fits like those shown in Figure 13d when an increasing number of modeling parameter sets are sampled instead of being set to their maximum likelihood values. The year chosen for display in Table VII is 2160, where the spread in projected temperatures is not rapidly changing. The top entry in Table VII is for sampling the development model parameters only, and for each such sample finding and using the maximum likelihood fits for all other parameters. Table VII shows that there is an increase from 1% to 18% of the total temperature projection uncertainty when also sampling the uncertainty in future break points and changes in the slope of carbon intensity of energy production vs. cumulative carbon use. Also sampling how the calibrated slopes for most recent data extrapolates into the future raises this number to 23%. In addition sampling the parameters in the atmospheric carbon balance model still only increases this number to 27%. Evidently the predominant contribution to the uncertainty comes from the atmospheric heat balance model—an unsurprising result given that the data used to calibrate this model has by far the largest variability. The result shown in Figure 14 is to be taken as one of the model used here as a whole, because this result is not reproduced if sampling of the probability distribution for the parameters in the atmospheric heat balance is replaced by use of their maximum likelihood values. A larger growth in spread of global average temperatures with its increase would not be a surprising result if a more complete model of the atmospheric heat balance with a greater number of a priori uncertain parameters were used. The method of plotting this result illustrated in Figure 14 is nevertheless potentially useful, since such a plot can concentrate the results for all future times of interest on a single plot with a horizontal axis of finite range.

TABLE VII

Contributions to temperature uncertainty in 2160

Varied	% of temperature spread
development index	1
+ intensity future	18
+ also intensity history	23
+ also CO ₂ balance	27
+ also heat balance	100

It is to be expected that the uncertainty in future carbon intensity has less important implications for shorter term extrapolations. For example, for the year 2110 the difference between also sampling the future changes in carbon intensity slope and just sampling the development index parameters accounts for 10% instead of Table VII's (18-1)%=17% of the total temperature projection uncertainty. For 2060 this difference is only 1%, and sampling all parameters but those in the atmospheric heat balance models accounts for only 13% of

the temperature projection uncertainty. Thus, especially for such shorter term projections, more careful modeling of the atmospheric heat balance than undertaken here is the highest priority for reducing uncertainties in projections of global average temperature.

All of the projection uncertainties discussed above are in the expected values of the indicated data sets (e.g. biennial or triennial averages). In addition there is an approximately normally distributed variation around the expected values for any scenario. As can be seen from Figures 1, and 4–7, this additional scatter is generally small except for about $\pm 0.1^\circ\text{C}$ in the case of biennial averages of global average temperature. At the global level this random fluctuation is small, although at finer geographical scale the results of climate fluctuations can be important even if they average out over a few years.

5. Conclusions and Extensions

The primary conclusion from this work is that it is possible to use econometric time-series analysis to produce systematically derived probability distributions to support projections of fossil carbon emissions. These can then be combined with similarly time-series-calibrated and sampled climate models to produce systematic projections of atmospheric carbon loading and climate parameters. Here the econometric analysis is done with a reasonably complete but still analytically tractable model of the evolution of labor supply, production efficiency, primary energy production, and fossil carbon use. While the global disaggregation is done only at the next highest level below a unified global analysis, this produces the interesting result that there is as yet no empirical motivation for the idea that the larger populations in developing countries are in the process of evolving towards a per capita rate of fossil carbon use comparable to that of developed countries. In this sense these two types of economies appear to be conditionally convergent (following patterns describable by the same equations) but not absolutely convergent in the sense of evolving to nearly the same per capita GDP or per capita energy or carbon use rates.

To conduct a study like this, there are inevitable compromises that have to be made between completeness and efficiency (c.f. Nordhaus and Boyer, 2000). Three major simplifications have been made here for the sake of efficiency. Chief among these simplifications is the choice of the saturating bootstrap model $\dot{a} = \nu a(1 - a)$ for a development index, which is used as an independent variable in place of time for the utility optimization part of the calculations. Through this choice and the analytic expansion of the Euler-Lagrange equations for utility optimization outlined in the Appendix, all time is mapped onto the unit interval $0 < a < 1$ for the independent variable. The different adjustable coefficients of $(\ln a)$ for each region in the log-linear production functions for primary energy and GDP take advantage of the expectation that the development index can be calibrated against population growth rates, without assuming an overly rigid connection between population growth rates and production efficiency.

A second major simplification is the use of a simple linear dependence of the additional energy production efficiency factor p on carbon intensity to de-

scribe the effects of fossil fuel depletion and the increasing marketization of diseconomies with cumulative fossil carbon use. A piecewise linear model ties the carbon intensity of energy use to cumulative carbon use with a connection to a data-calibrated slope break at the end of the historical “age of coal,” after which economies became petroleum dominated. Samples for fits to historical data on carbon intensity are projected forward until energy de-carbonization slows down during a “new age of coal” because it is difficult to reduce the average carbon intensity below a value corresponding to heavy use of natural gas. A more complete model of carbon intensity would be based on detailed multidisciplinary study of the evolution of the policymaking framework that shapes decisions on such matters.

A third simplification is that, at least for the present application, the solutions to the resulting Euler-Lagrange equations have been expanded in three sets of parameters: the capital fraction of energy, the ratio of the fossil carbon depletion rate to the capitalization time, and the ratio of the development rate to the capitalization time. Of these only the last is a significant concern with respect to the balance between computational accuracy and the applicability of the overall formulation, so expansion in this “capitalization lag” is taken to one higher order than for the other expansions. For more detailed studies, particularly where rapidly growing economies like China’s are treated as separate regions, numerical integration of the effect of the capitalization lag is both desirable and feasible.

One more simplification adopted is the technique of subtracting out preindustrial base values before doing time-series calibration, and then adding them back in to final modeling results for plotting purposes. This approach allows results to be extrapolated arbitrarily far backward as well as forward in time without obtaining physically nonsensical results. Of course, extreme extrapolations either forward or backward in time will enter realms where the set of models used here cannot be expected to be applicable. In the distant future, for example, population may not approach a steady level near that projected. Population could gradually decline over an extended period of less than replacement fertility rates, or it could increase due to greater longevity or a long period of exponential growth of what are now small sub-populations in developed countries. Also, the atmospheric response model used here does not account for very long term mixing into deep oceans or ice sheet melting.

For the distant past, the early-time $a \rightarrow 0$ regularity boundary conditions used here are only an approximation that is adequate for a number of capitalization times after major economic disruptions. For quantitative comparison with earlier data, appropriate models of punctuated destruction of capital and labor would need to be added, though with these included the utility optimization approach adopted here can track the recovery from such disruptions using numerical integration. An interesting phenomenon observed in preliminary studies of this type is an overshoot of the background GDP trend, followed by a damped oscillation around it.

The historical observation of significant departures from the smoothly evolving trends and multiply periodic variations around them occurring not long be-

fore the time range of data used fitting and extrapolation in the present study is precautionary. This observation suggests that including probability distributions for such disruptions in the future would be worthwhile to illuminate how much broader the spread in outcomes from a more realistic model would be. One obvious choice is to include a stochastic model of volcanic eruptions, based on historical data. Other possibilities noted above as not included in the present analysis include major wars, pandemics, and breakdowns in economic functioning on the scale of China's "Great Leap." There is considerable a priori uncertainty in the probability and scale of such occurrences, but at least there are historical time-series data available to calibrate probability distributions for parameters important in modeling how economies have reacted to such disruptions. A project currently in progress should provide a broader and more finely geographically resolved set of background data on international energy production and trade in support of such studies (Rethinaraj and Singer, 2007).

To the extent that their effects extrapolate smoothly into the future, gradual progress in technology and social organization that allows increasing productivity and adoption of less carbon intensive energy production is implicitly accounted for in the present approach. However, major technological innovations have significantly perturbed established patterns of energy and fossil carbon use in the past. Examples include the widespread adoption of the use of coal in steam engines, and the adoption of technology for drilling water wells to the extraction of fluid fossil fuels. The possibility of such future dramatic developments can be allowed for within the context of the present approach, for example by basing probability distributions for future changes in the slope of the carbon intensity of energy production on detailed analysis of physical constraints on energy technologies and detailed studies of market response to new technological innovations. Based on current knowledge there is a large a priori uncertainty concerning when dramatic technological breakthroughs might occur and how much impact they will have, so allowing for such possibilities should increase the spread of outcomes for global carbon emissions and their consequences. Here, the focus has just been on developing a convenient methodology for folding information from historical time-series data into such analyses. The samples of changes in the slope of carbon intensity as a function of cumulative carbon shown in Figure 8 offer a single illustrative example of how this can be generalized beyond just extrapolating historical trends.

For the level of analysis in this paper, there are four major motivations for combining an analytically solvable model of utility maximization with atmospheric response models whose solutions can be expressed in the form of the integrals described in the Appendix. First, all of the results to be compared with data can be computed readily using either power series expansions or other well-known and readily available computation methods for the one required hypergeometric function. Second, all the integrals required for data calibration can be expressed analytically or as sums of contributions of data points to quadratures. This avoids the need to imbed, within the calibration procedures, Runge-Kutta-type integrations (Press, 1986) or coarsely gridded integral-form utility optimizations using software such as the General Algebraic Modeling

System (GAMS). Third, all of the formulas used are analytically differentiable, which streamlines the formulation of searches for maximum likelihood points. This feature also facilitates finding the second derivatives of likelihood used in constructing exact and approximate multivariate t-distribution approximations to various posterior probability distributions in support of random sampling of a priori uncertain parameters. Fourth and finally, with careful examination the physical meaning of analytic formulas is more apparent than solutions that can only be found through finite difference techniques or through gridded integral maximization procedures. Moreover, whether expanded analytically or not, the differential Euler-Lagrange formulation easily lends itself to solution on the finest desired timescales for comparison even to annual time-series data. This is particularly helpful when combining the secular evolution of functions of time with periodic corrections in order to come up with overall models whose differences from data are indistinguishable from iid according to the statistical tests used.

Even the remaining complexity in the present model could be avoided by using a more empirically and less theoretically grounded approach. However, there are both conceptual and practical advantages to putting up with the complexity imposed by the choice of a dynamic optimization approach. The conceptual advantage is that each piece of the secular model is anchored to an underlying hypothesis whose applicability is econometrically tied to data. In some cases, such as the saturating bootstrap model $\dot{a} = \nu a(1-a)$ for the development index, the underlying model is extremely simple and in this case functionally equivalent to the empirical choice of a logistic function. In this particular case, the challenge of theory formulation is comparable to the difficulty that any complete model of economic development has in dealing with “social capital.” This is the important but difficult to directly measure combination of rule of law and other societal factors that allow for economic recovery on a capitalization timescale from the most devastating disruptions in developed countries. In other cases, such as for the model used for dependence of carbon intensity on cumulative carbon use, the “theory” adopted is only loosely tied to environmental concerns and could use considerable improvement as described below. Also, purely empirical formulas have been used here for the modest but not always negligible periodic corrections to the secular trends computed from the theoretical model. Ideally these non-secular corrections would also be based on theoretical models of relevant processes such as business cycles and energy cartel stability. Nevertheless, the adoption of a reasonably complete and empirically adequate model for secular trends, with periodic corrections that correlate in meaningful way with historical events, provides a potentially useful starting point for extending and refining the analysis without reliance on proliferation of an increasing number of arbitrary empirical modeling parameters.

A question of immediate interest that can be examined with the model described here is how projection uncertainty can be expected to decline with accumulating experience. This question can be addressed by using the present model to produce synthetic projected data sets, and then combining the entire accumulated time-series “data” to reproduce the analysis of projection uncertainty.

The reason this is interesting is that the level of uncertainty can have an important impact on policymaking, allowing some to call for action on the grounds of risk reduction and others to insist on waiting until more accurate projections become available. In this context it would be particularly interesting to couple the type of econometric analysis described above with more complete atmospheric carbon and heat balance models and a more theoretically grounded analysis of the interaction between policy choices influencing the level of carbon emissions with the evolution of climate parameters. One way to approach this is to include the effect of climate modification on economic production and then repeat utility optimization jointly vs. separately with respect to fossil carbon utilization. Under the hypothesis that a given level of global per capita benefit is needed to overcome vested interests resisting effective action to reduce carbon emissions, a more complete analytic theory of probability distributions for future carbon emissions and climate effects could then be developed. In this context it would also be desirable to use a finer level of disaggregation to support game theory modeling of the distribution of the benefits of cooperative action amongst major negotiating blocks (c.f. Ipsen et al., 2001). Preliminary studies with the present model using eleven groups of countries sometimes used in Intergovernmental Panel on Climate Change (IPCC, 2001) studies suggest that this is tractable, although it may require revisiting numerical integration of the Euler-Lagrange equations for utility maximization in the case of economies like China that have experienced rapid economic growth and concomitant substantial capitalization lags.

Finally, in a related work, the overall past and future energy production has been computed for time-series calibrated subdivision of primary energy into competing pairs of primary energy sources (Rethinaraj, 2005). These include fluid fossil fuels, coal, water-driven electricity production, wind and solar thermal electricity production, and the competition between various sources of nuclear fuel. Such analysis can complement the kind of extensions suggested here by providing insight into the practicality at a more detailed level of making the asymptotic approach to non-fossil economies that is both physically unavoidable and intrinsic to the approach used in this paper. The relatively complete but analytically tractable theoretical framework and the extensive and flexible database developed to support the results presented in this paper should provide a sound basis for such work.

Appendix. Derivations and Computations

This appendix first provides an outline of expansion methods for solving Euler-Lagrange equations for utility optimization. More details can be found in Rethinaraaj (2005). The methods used in a series of computational modules for sampling probability distributions are then described.

The integral of total discounted per capita utility of consumption is maximized subject to the material balance constraint for carbon utilization. In dimensionless variables, the material balance constraint for each region is $\dot{u} = \epsilon fw$, where u is the ratio of cumulative carbon utilization to its long-term limit value, f is the ratio of the carbon intensity of energy production to its initial value, w is the ratio of energy use rate to its long term limit value, and ϵ is a different constant in each region of piecewise linear fit to the dependence on carbon intensity to cumulative carbon use. Defining

$$\mathcal{L} = a^\theta e^{-\rho t} C^{1-\theta} / (1 - \theta) + \kappa \beta a^\theta e^{-\rho t} C^{-\theta} (fw - \dot{u}/\epsilon)$$

the control variables $\{k, l, f, u, K\}$ and the Lagrange multiplier κ are determined by the Euler-Lagrange equations

$$0 = \frac{\delta \mathcal{L}}{\delta k} = \frac{\delta \mathcal{L}}{\delta l} = \frac{\delta \mathcal{L}}{\delta f} = \frac{\delta \mathcal{L}}{\delta u} - \frac{d}{dt} \left(\frac{\delta \mathcal{L}}{\delta \dot{u}} \right) = \frac{\delta \mathcal{L}}{\delta K} - \frac{d}{dt} \left(\frac{\delta \mathcal{L}}{\delta \dot{K}} \right) = \frac{\delta \mathcal{L}}{\delta \kappa}$$

The constraint $\dot{u} = \epsilon fw$ also requires $\beta a^\theta e^{-\rho t} C^{-\theta} (fw - \dot{u}/\epsilon) = 0$, and when the constraint is written in this form the resulting differential equations are more compact. The equations $\delta \mathcal{L}/\delta k = \delta \mathcal{L}/\delta l = 0$ give the exact result $k = l$.

The next step is to show that to lowest order in both ϵ and β we have $k = 1$, and thus $l = 1$. Multiplying the Euler-Lagrange equation $\delta \mathcal{L}/\delta u = d(\delta \mathcal{L}/\delta \dot{u})/dt$ by $(\epsilon/\beta)K^{-1}e^{\rho t}a^{-\theta}C^\theta$ gives

$$\begin{aligned} (\epsilon/\beta)K^{-1}e^{\rho t}a^{-\theta}C^\theta (\delta \mathcal{L}/\delta C)(\delta C/\delta Y)Y \delta \ln Y/\delta u - (\kappa/K)\delta(fw)/\delta u \\ = K^{-1}e^{\rho t}a^{-\theta}C^\theta d(Ke^{-\rho t}a^\theta C^{-\theta} \kappa/K)/dt \end{aligned}$$

Noting that $\delta \ln Y/\delta u = \beta \delta \ln p/\delta u$ and that the remaining terms multiplying (ϵ/β) on the right hand side are of order 1, it can be seen that $\kappa/K \sim \epsilon$. This means that the correction containing the factor κ/K in the $\delta \mathcal{L}/\delta u = d(\delta \mathcal{L}/\delta \dot{u})/dt$ equation, $-\varphi(k/F)/(1 - \beta k) + 1/F - \alpha(\kappa/K)fw = 0$, is of order ϵ . Thus to lowest order in both ϵ and β we have $k = 1$.

The expansion in the small capital fraction of energy, β , is very useful because the solution for GDP to lowest order can be obtained separately from the rest of the problem and the result is sufficient for the rest of the analysis. Define a function $F = K/Y$ proportional to the capital intensity of production and a function $G = (\alpha^{-1} - r)K/C$ proportional to the capital intensity of consumption. Multiplying the Euler-Lagrange equation $\delta \mathcal{L}/\delta K = d(\delta \mathcal{L}/\delta \dot{K})/dt$ by $e^{\rho t}a^{-\theta}C^\theta$ gives, to lowest order in β , with $G' = dG/da$ and $F' = dF/da$,

$$\begin{aligned} -z\delta(1 + \delta)FG - \delta\eta^{-1}z(1 + \delta)F'G + \delta\eta^{-1}\omega^{-1}zG'(1 + \delta)F \\ = (1 + \delta)FG - (1 + \delta)G \end{aligned}$$

$$\begin{aligned} \alpha^{-1}G - r(1 + \delta)FG - (1 + \eta/\omega)\nu z(1 + \delta)FG + \delta\omega^{-1}\eta^{-1}\theta^{-1}(1 + \delta)F'G \\ = (\alpha^{-1} - r)(1 + \delta)F \end{aligned}$$

These equations can algebraically be solved iteratively for coefficients to any order in series expansions in δ . The result of interest here is

$$F \approx (1 + a\delta + az\gamma_2\delta^2) / (1 + \delta)$$

where $\gamma_2 = 1 + \xi/\omega + \gamma_1(1 - \xi^{-1})$ and $\gamma_1 = (1 - (1 + \xi^{-1})/\theta)(\alpha^{-1} - r)$. Including division by the factor $1 + \delta$ in the result for F gives it the very useful property that the resulting series exactly satisfies regularity boundary conditions at early time ($a \rightarrow 0$) and large time ($z = 1 - a \rightarrow 0$) if at least the first order approximation terms $F_1 = (1 + a\delta)/(1 + \delta)$ are retained. This expansion is only asymptotically convergent, and we do not find it useful to keep more terms than included in F_1 . However, in Table II we do report the maximum value $\gamma_2(\delta/2)^2$ of $az\gamma_2\delta^2$ to give an idea of the size of the omitted terms.

It remains to integrate the fossil carbon balance constraint $\dot{u} = \epsilon_k f w$ over each of the piecewise linear portions of the dependence of carbon intensity on cumulative carbon use. For model projections and historical data fitting, this is done starting from a reference point a_4 where the integrated carbon use in dimensional terms is known from the carbon intensity fitting procedure described below. The result for the historical data fitting done here is given in the main text in terms of

$$S[a] = \int_0^a da a^\psi (1 + a\delta)^{\alpha/\omega} / (za) = \text{AppellF1}[\psi, -\alpha/\omega, 1, \psi + 1, -a\delta, a]$$

Here, with $(d)_n = d(d+1) \dots (d+n-1)$ for any quantity d , the hypergeometric function on the right hand side of this equation is (Wolfram, 2003)

$$\sum_{m=0}^{\infty} \sum_{n=0}^{\infty} (-a\delta)^m a^n (\psi)_{m+n} (-\alpha/\omega)_m (1)_n / (m!n!(\psi+1)_{m+n})$$

For repeated calculation of $\text{AppellF1}[\psi, -\alpha/\omega, 1, \psi + 1, a\delta, a]$ at fixed values of a and δ over a narrow range of ψ , it is convenient to expand this result as a third order Taylor series around a reference value of ψ . This reference value is taken to be the maximum likelihood value for the probability distribution for which it is being calculated.

Next we describe the sampling methods used to produce the results in the main text. After a general introduction, to give an idea of the modularity of the approach used, each such description is preceded by the name of the *Mathematica* notebook (Wolfram, 2003) used to execute it.

First we note that periodic corrections to secular fits are done only after data with even spacing along the abscissa are first prepared. Following Wei (1979, pp. 261-62), we halve the number n of data points and round down to the nearest integer to obtain $n_2 = \lfloor n/2 \rfloor$. For frequencies $\mathcal{F}_k = 2\pi k/n$ with $1 \leq k \leq n_2$, let \bar{e}_m be the residuals between the uncorrected fit and the data and the Fourier amplitudes be $\bar{B}_k = (2/n) \sum_{m=1}^n \bar{e}_m \cos[m\mathcal{F}_k]$ and $\bar{A}_k = (2/n) \sum_{m=1}^n \bar{e}_m \sin[m\mathcal{F}_k]$

for $k = 1 \dots n_2$, except that $\bar{\mathcal{A}}_{n_2} = (1/n) \sum_{m=1}^n \bar{e}_m \cos[m\mathcal{F}_k]$ if n is even. (Here and below, k is a dummy index, not the energy sector capital parameter.) The periodicity amplitudes are $\bar{\mathcal{P}}_k = (n/2)(\bar{\mathcal{A}}_k^2 + \bar{\mathcal{B}}_k^2)$ except that $\bar{\mathcal{P}}_{n_2} = n\bar{\mathcal{A}}_{n_2}^2$ if n is even. Ordering these in a sequence $\bar{\mathcal{P}}_j$ of decreasing size with increasing index j , Wei notes that the significance criterion for each amplitude is to an excellent approximation $(\nu_{\text{free}} + 1 - j)(1 - \tau_j)^{\nu_{\text{free}} - j}$ where $\tau_j = \bar{\mathcal{P}}_j / ((\sum_{m=1}^{n_2} \bar{\mathcal{P}}_m) - (\sum_{m=1}^j \bar{\mathcal{P}}_m))$. Here $\nu_{\text{free}} = n - M$ where M is the number of parameters in the fit. The test used for significance of nearest neighbor correlation is $\sum_{m=1}^{n-1} \bar{D}_m \bar{D}_{m+1} / \sum_{m=1}^n \bar{D}_m^2$, where \bar{D}_m are the residuals between the data and the fits, with the fits including periodicity corrections where applicable (Wei 1979, p. 23). Generalizing these analyses to the set of eleven presumably independent time series used here, we require that each of these minimum values of for these statistical tests is greater than $1 - (1/2)^{1/11} = 0.061$.

Another generic comment concerns three types of methods used for sampling parameters in which models are respectively linear, nearly linear, or not nearly linear (“fully nonlinear”). In all cases, what is of interest here is the marginal probability distribution integrated over the standard deviation describing the spread of the data around the theory result.

For linear parameters the result is a multivariate-t distribution, whose covariance matrix is designated as $X'X$ by Box and Tiao (1973, 115). Such parameters are sampled by using the singular value decomposition of the covariance matrix to construct a linear transformation of independent variables that makes the probability distribution circularly or hyperspherically symmetric about the origin. The radial variable then has a F distribution that can be analytically sampled (Box and Tiao, 1973, 117). With only one additional variable, the circular angle of the resulting circle is uniformly sampled. The other cases encountered here have more than two additional variables, for which the surface of the resulting unit hypersphere has rectangular coordinates $(\cos \zeta_0) \prod_{k=1}^K \sin \zeta_k$ for values of K up to two less than the total number of parameters. In such cases ζ_0 is sampled uniformly from 0 to 2π and the cumulative distribution function for $(\sin \zeta_k)^k$ is uniformly sampled for each k up to and including K by the “transformation method.” This method involves simply setting each such normalized cumulative distribution function to a uniform random number from the unit interval and solving numerically for the corresponding value of ζ_k (as in Press et al., 1986, Section 7.2).

For nearly linear parameters we use a generalization of the rejection method described by Press et al. (1986, Section 7.3). In principle this can be done by choosing random locations covering the entire area like that including the points shown in Figure 3, and then rejecting samples for which a pseudo-random (hereafter “random”) number from the unit interval is less than

$$\int_{-\infty}^{\infty} d(\ln[\sigma]) \prod_{j=1}^n \left(2\pi e^{2\ln[\sigma]}\right)^{-n/2} e^{-(\delta_j/e^{\ln[\sigma]})^2/2}$$

where the δ_j are the residual differences between the data and the theory (c.f. Press et al, 1986, Section 7.3). This integral is the probability of the data

given the theory, integrated over the a priori unknown standard deviation σ , under the assumption that there is no prior information about the value of $\ln \sigma$. (There is by contrast always prior information available about σ since it is positive definite, as noted in standard statistical reference works such as Box and Tiao, 1972.) In practice the area over which this integral is appreciable covers only a thin swatch of parameter space, so an efficient rejection sampling technique requires a reasonable analytic approximation to this integral as a starting point. This approximation uses the $(2m + 2) \times (2m + 2)$ covariance matrix for a multivariate student's t distribution as a starting point, where, for example, the number of different periodic corrections to the logistic functions described in the legend to Figure 1 is $m = 2$ for the tropical region and $m = 5$ for the temperate region.

In the approach used here, an approximate probability distribution is first obtained by expanding the sum of the squares of the residuals between data and theory as a power series around the maximum likelihood values of the relevant parameters and including only the quadratic terms. This resulting "Hessian" approximation yields a probability distribution that is multiplied by a number large enough to make it everywhere just equal to or larger than the exact probability distribution for all of the samples ultimately chosen. The approximate distribution is sampled as described in the previous paragraph, and such samples are accepted if and only the ratio of the exact to approximate probabilities at the sampling point is greater than a random number chosen uniformly from the unit interval.

For fully nonlinear parameters, a marginal probability distribution is first obtained by analytically integrating over the linear parameters (Box and Tiao, 1979, pp. 145–146). Then cubic spline fits to samples spaced at one seventh or more of the sampled range are obtained over the "region of interest" for the rest of the parameters. The result is integrated over all but one parameter, which is then sampled by the above-mentioned "transformation method." For this sample, the process is repeated for the remaining nonlinear parameters one at a time; and when this is completed the linear parameters are sampled as described above. The "region of interest" is that for which the probability of a sample is at least a minimum value of interest, here taken to be 0.001 or less. Where adjustable multipliers of the periodic corrections frequencies picked out by discrete Fourier power spectrum analysis are included, these are sampled only within a specified unit range, as described below for the cases of fossil carbon use and the atmospheric heat balance. The spline fits just described are also extremized to find starting points for the maximum likelihood parameter searches, for which the linear parameter optima are first eliminated analytically. (For nearly linear cases the spline fit is not necessary because the linear approximation can be used to find an analytically determined starting point for the maximum likelihood search). In some cases analytic elimination of linear parameters yields formulas that are too cumbersome for the built-in *Mathematica* software to find a maximum likelihood. In such cases, the sum of squares of residuals minimized over the other parameters is surveyed and fit

with a quadratic function of the remaining parameter in the neighborhood of its optimum value in order to pinpoint the optimal value.

GLOBAL: The parameters assumed to be global universal constants are the capital fraction of production α , the inverse θ of the intertemporal substitutability of consumption, the capital depreciation rate \bar{r} , and the pure rate of time preference $\bar{\rho}$. It is actually the labor fraction of production $\omega = 1 - \alpha$ that is estimated from data on labor fraction of compensation (Gollin, 2002). What are appropriate methods for derivation and appropriate application of probability distributions for some of these parameters is a question not without controversy, as discussed for example by Füssel (2007). The approach taken here is to be as transparent as possible about the data bases and methods used, leaving the reader to decide whether these or alternative approaches are the most useful for any particular application.

Early estimates of the intertemporal substitutability of consumption from data on returns on investment gave both large and highly varied estimates of its inverse (c.f. Hall, 1988). Ogaki and Reinhart (1998) critiqued the methods used by Hall and others (Hansen and Singleton, 1996) and estimated values for $1/\theta$ of 0.329–0.447 depending on the values of other parameters in the analysis, based on post-WWII data through 1983 for the United States. As detailed below in the subsection on estimation of θ below, it is instead estimated here from a regression of international survey data on “happiness” and “satisfaction” (Myers and Diener, 1995). We took from this survey the average of responses on the same numerical scale for ratings of happiness and satisfaction for countries other than reforming communist ones and did a regression against per capita income as detailed below. Reforming communist countries were omitted on the grounds of being far from equilibrium, since they reported an anomalously low response that was much lower than before the collapse of the Soviet Union where data was available.

In principle the survey data of Myers and Diener could give a direct measure of how utility relates to per capita consumption. In practice the estimation method used here also raises many questions (c.f. Füssel, 2007). Are the answers to questions posed in different languages are really commensurate and representative of what economic decisions attempt to discount and maximize? Have other important hidden variables been neglected, even after rejection of clearly anomalous non-equilibrium results data from reforming communist economies? While the method used here assumes that the responses to the survey questions are a measure of what decisions on use of production are attempting to maximize, the idea that per capita consumption taken to some power is also a useful measure of what decisions on used of production are attempting to maximize is also just an assumption. Any such assumption is a matter of conjecture, with the primary practical question of interest here being whether the resulting model is functionally useful. The method adopted here for estimation of θ is chosen on the basis of transparency of its ease of implementation and the global reach of of the data used. The result can be readily related to previous literature in that it gives an estimate comparable to if somewhat larger than the value $\theta = 1$

assumed, for example, by Nordhaus (1944) and by Manne et al. (1995), and not so much smaller than that inferred by Ogaki and Reinhart from data from financial data from the United States as to have a critically important impact on the overall model results of primary interest here. The reason for this is that θ affects the results of interest here only to first order in the expansion parameter $\delta = \theta\xi\nu$. However, we do note that doubling θ from the maximum likelihood estimate of 1.345 obtained here would increase the largest value of $\gamma_2(\delta/2)^2$ of the second order capitalization lag correction, for the temperate region, from nearly 0.1 to nearly 0.4. Inclusion of the factor $(1 + \delta)$ in the denominator when analytically expanding the capitalization lag F , is a help in this regard, because, by making the approximation $F_1 = (1 + \delta a)/(1 + \delta)$ exactly fit the boundary conditions, it makes this approximation close to the exact numerical solution even when the first order correction δa is not small. Nevertheless, that numerical integration of the Euler-Lagrange equations should be examined if values of θ this large enough to make $\gamma_2(\delta/2)^2 \sim 0.4$ are thought to be relevant.

Useful data of global coverage was difficult to come by for the capital depreciation rate. Since the capital depreciation rate \bar{r} is also taken to be a universal constant, it was estimated as described below from time-series data available for the United States (Bishoff and Kokkelenberg, 1987). However, we note a recent report leading to a value of 0.14/yr for geometric mean of depreciation estimates from five tropical region countries (Côte d'Ivoire, Ghan, Kenya, Zimbabwe, and the Philippines, from Bu, 2006). This is larger than other estimates based on developing countries of 0.04/yr (Nehru and Dhareshwar, 1993) to 0.07/yr (Easterly and Rebelo, 1993). The $\Delta V/V$ value for \bar{r} given in Table I is derived only from a single data set and thus should be understood as being smaller than what would likely result from a more internationally based approach. The data chosen for the present study before the availability the results from Bu (2006) led to an estimate for \bar{r} that somewhat fortuitously lies in between Bu's results for developing countries and the above-mentioned results based on information from developed countries. We do take note that Bu (2006) points out how using a universal depreciation rate may not be the most appropriate approach for studies involving both developed and developing countries. This suggests that allowing for a dependence of the depreciation rate on the development index might be eventually be desirable. Since the depreciation rate \bar{r} only affects the results here through a correction of first order in the capitalization lag, $\delta = \theta\xi\bar{\nu}/(\bar{r} + \bar{\rho})$, we have not delved into such complications here.

It would also not be surprising if the pure time rate of preference $\bar{\rho}$ also depended on development (c.f. Rao, 2000). Preliminary studies indicate that it is mathematically tractable to allow $\bar{\rho}$ to be linear function of the development index. Again, however, since the value of $\bar{\rho}$ also only affects the results of primary interest here through a correction of first order in the capitalization lag, $\delta = \theta\xi\bar{\nu}/(\bar{r} + \bar{\rho})$, the additional complications that such an approach would bring did not seem necessarily for the present study. Thus, based on a theory derived from work of Ramsey (1928) and described for example by Barro and Sala-i-Martin (1995, Section 2.1), a universal constant pure rate of time preference is estimated from data on the differences between inflation-adjusted interest rate

and θ times the rate of growth of per capita income (WDI, 2005). Details of these various calculations are as follows:

α : The complement $\alpha=1-\omega$ of the estimates of the labor shares of compensation for $n_\alpha = 31$ countries (Gollin, 2002) are assumed to have a Beta distribution, i.e. proportional to $\alpha^{R_\alpha-1}\omega^{S_\alpha-1}$. The estimator used for α is simply the mean $\langle \alpha \rangle$ of the data for α . Estimators \hat{R} and \hat{S} for R_α and S_α satisfy $\langle \ln[\alpha] \rangle = \Psi[\hat{R}] - \Psi[\hat{R} + \hat{S}]$ and $\langle \ln[\omega] \rangle = \Psi[\hat{S}] - \Psi[\hat{R} + \hat{S}]$ where $\Psi[x] = d \ln \Gamma / dx$ and $\Gamma[x+1] = x\Gamma[x]$ defines $\Gamma[x]$. Also following Bickel and Doksum (1977, p. 44) the “spread” reported in Table I is $(\hat{R}\hat{S}(\hat{R} + \hat{S})^2(\hat{R} + \hat{S} + 1))^{1/2}$.

$\hat{\theta}$: An estimate $\hat{\theta} = 1 - \hat{m}_\theta$ for the inverse of the intertemporal substitutability of consumption is obtained from a least squares fit of the form $\ln[(100 - \text{wellbeing})/100] = m_\theta \ln[\text{wealth}/1000] + b_\theta$ to a set of $n_\theta = 41$ estimates of self-reported “wellbeing” as a function of average per capita income (“wealth”) for all countries for which data was available (Myers and Diener, 1995; Maddison, 2001; Rethinaraj, 2005), with the exception of reforming communist countries for which the reported “wellbeing” is taken to reflect an unusual situation far from equilibrium. Here “wellbeing” is the average of levels of “happiness” and “satisfaction.” The marginal distribution for θ integrated over b_θ is assumed to have a student-t distribution with $n_\theta-2$ degrees of freedom.

\tilde{r} : A time series \tilde{r}_j for $j=1\dots n_r=31$ annual estimates the overall capital depreciation rate for the United States (Bischoff and Kokkelenberg, 1987) is assumed to have residuals independently and identically distributed around the values $\hat{r} + \hat{\theta}_1 \cos[\pi(N_r j/n_r)] + \hat{\theta}_2 \sin[2\pi(N_r j/n_r)]$ for some constants $\hat{\theta}_1$ and $\hat{\theta}_2$. Here $N_r = 2$ is the dominant amplitude of the finite Fourier decomposition of the difference between the \tilde{r}_j and their mean value. The marginal distribution for \tilde{r} has a student-t distribution with $n_r - 3$ degrees of freedom.

$\bar{\rho}$: The estimate of the pure rate of time preference used here follows an analytic rather than normative approach. That is, observational data is used insofar as possible to calibrate a well established model, rather than imposing a normatively chosen value. To make this clear, the model used here is described in some detail. Following a model of utility maximization of the utility of per capital household income described by Barro and Sala-i-Martin (2004, Section 2.1) and motivated by earlier work of Ramsey (1928), the pure rate of time preference is estimated from real interest rates less θ times growth rates of per capita gross domestic product. The real interest rate is the nominal lending rate less the rate of inflation. For cases with high inflation rates this involves taking the difference of two large numbers. On the assumption that the values of these numbers are distributed with common variance, it is thus approximately appropriate to weight the contribution from each pair thereof by the inverse of the square of the inflation rate. The data on lending and inflation rates comes from the World Bank (WDI, 2005), and economic growth rates are computed from data from Maddison (2001). Under these assumptions, the probability distribution for one observation can be rewritten as $\left(2\pi\bar{\sigma}_\rho^2\tilde{W}_j^2\right)^{-1/2} \exp[-(\tilde{y}_j - \bar{\rho})^2 / (2\bar{\sigma}_\rho^2\tilde{W}_j^2)]$. Here the elements of a vector $\tilde{\mathbf{y}}$ are $\tilde{y}_j = \tilde{\mathfrak{R}}_j - \hat{\theta}\tilde{g}_j$, where $\tilde{\mathfrak{R}}_j$ are real interest rates and \tilde{g}_j refers to the rates frac-

tional annual growth in GDP. Multiplying these distributions gives the result $L(\bar{\rho}, \bar{\sigma}_\rho | \tilde{\mathbf{y}}) = \left(1 / \prod_{j=1}^{n_\rho} (2\pi \bar{\sigma}_\rho^2 \tilde{W}_j^2)^{1/2}\right) \exp \left[- \sum_{j=1}^{n_\rho} \left((\tilde{y}_j - \bar{\rho}) / \tilde{W}_j \right)^2 / (2\bar{\sigma}_\rho^2) \right]$. Following Box and Tiao (1972), this is multiplied by a prior probability distribution for $\bar{\sigma}_\rho$ proportional to $1/\bar{\sigma}_\rho$ to obtain the posterior probability distribution $P(\bar{\rho}, \bar{\sigma}_\rho | \tilde{\mathbf{y}})$ for the data given the vector $\tilde{\mathbf{y}}$ of data from which an estimate $\hat{\rho}$ is to be found. Maximizing with respect to $\bar{\rho}$ gives the weighted estimate $\hat{\rho} = \left(\sum_{j=1}^{n_\rho} (\tilde{y}_j / \tilde{W}_j) \right) / \left(\sum_{j=1}^{n_\rho} (1 / \tilde{W}_j) \right)$. What we are interested in here is the marginal distribution for $\bar{\rho}$ integrated over the “nuisance parameter” $\bar{\sigma}_\rho$. Generalizing the derivation of Box and Tiao to this weighted case, note that $\sum_{j=1}^{n_\rho} \left((\tilde{y}_j - \bar{\rho}) / \tilde{W}_j \right)^2 = \sum_{j=1}^{n_\rho} \left((\tilde{y}_j - \hat{\rho}) / \tilde{W}_j \right)^2 + (\tilde{y}_j - \hat{\rho})^2 \sum_{j=1}^{n_\rho} (1 / \tilde{W}_j)^2$. Defining $\bar{s}^2 = (1/\nu_\rho) (\sum_{j=1}^{n_\rho} (\tilde{y}_j - \hat{\rho})^2 / \tilde{W}_j^2) n_\rho / \sum_{j=1}^{n_\rho} (1 / \tilde{W}_j^2)$ where $\nu_\rho = n_\rho - 1$, we have that $P(\bar{\rho}, \bar{\sigma}_\rho | \tilde{\mathbf{y}}) = \bar{k}_\rho \bar{\sigma}_\rho^{-n_\rho-1} \exp[(\nu_\rho \bar{s}^2 + n_\rho (\bar{\rho} - \hat{\rho})^2) / (2\bar{\sigma}_\rho \bar{W}^2)]$ where we set $\bar{\sigma}_\rho \bar{W}^2 = \bar{\sigma}_\rho n_\rho / \sum_{j=1}^{n_\rho} (1 / \tilde{W}_j)^2$, and choose the constant \bar{k}_ρ to get the total probability to integrate to 1. Integrating this result over $\bar{\sigma}_\rho$ exactly follows the similar integration for the unweighted case as in Box and Tiao, thus giving a t-distribution for the marginal probability density for $\bar{\rho}$ integrated over $\bar{\sigma}_\rho$:

$$P(\bar{\rho} | \mathbf{y}) = \frac{\bar{s} / \sqrt{n_\rho}}{\text{Beta}[\nu_\rho / 2, 1/2] \sqrt{\nu_\rho}} \left[1 + \frac{n_\rho (\bar{\rho} - \hat{\rho})^2}{\nu_\rho \bar{s}^2} \right]^{-(\nu_\rho + 1)/2}$$

When n_ρ is very large, as in the case of interest here, this can be approximated by a normal distribution with mean $\hat{\rho}$ and variance \bar{s}^2 , whose square root is reported as the spread for this parameter.

DEVELOP: The logistic development index $a = 1 / (1 + \exp[-\bar{\nu}(\tilde{t} - \bar{t}_0)])$ increases approximately linearly with time near the inflection point where $a = 1/2$. The next term in the power series expansion around $a = 1/2$ that gives the linear approximation $a \approx 1/2 + (\tilde{t} - \bar{t}_0)\bar{\nu}/4$ is $-\bar{\nu}^3(\tilde{t} - \bar{t}_0)^3/48 \approx -(4/3)(a - 0.5)^3$. The population growth rate $\bar{\nu}z = \bar{\nu}(1 - a)$ used here to calibrate the logistic model parameters is thus usefully written in the form

$$\bar{\nu}z \approx \bar{\nu}/2 - (\tilde{t} - \bar{t}_0)(\bar{\nu}/2)^2 = \bar{\vartheta}_1 + \bar{\vartheta}_2 \tilde{t}$$

where $\bar{\vartheta}_2 = -(\bar{\nu}/2)^2$ and $\bar{\vartheta}_1 = (\bar{\nu}/2)(1 + \bar{t}_0\bar{\nu}/2)$, and thus $\bar{t}_0 = (2/\bar{\nu})(2\bar{\vartheta}_1/\bar{\nu} - 1)$ gives $\bar{\nu} = 2\sqrt{-\bar{\vartheta}_2}$ and $\bar{t}_0 = (\bar{\vartheta}_1/\sqrt{-\bar{\vartheta}_2} - 1)/\sqrt{-\bar{\vartheta}_2}$. Inserting these expressions into $\bar{\nu}z = \bar{\nu}(1 - 1/(1 + \exp[-\bar{\nu}(\tilde{t} - \bar{t}_0)]))$ gives a formulation for $d \ln[\bar{P}]/d\tilde{t}$ that can be fit with a function that is nearly linear in $\{\bar{\vartheta}_1, \bar{\vartheta}_2\}$ for a reasonably wide range around $a = 1/2$. The nearly linear fit in these variables is sampled as described above and then converted back to the variables whose values are reported herein.

GDP: The expression for the logarithmic derivative of GDP vs. development is $d \ln[\tilde{G}_{DP}]/da = 1 + \xi + (\alpha/\omega)d \ln F_1/da$. Here $F_1 = (1 + a\delta)/(1 + \delta)$ where $\delta = \nu\theta\xi$ with $\xi = \eta/\omega$. The logarithmic derivative $ad \ln F_1/da$ is of order the

ordering parameter δ , and $(d \ln \tilde{G}_{DP}/da - 1)$ is known once the calibrations and sampling described above are done. We thus have here a single-parameter regression that is nearly linear in ξ , so it is dealt with as described above for nearly linear cases.

INTENSITY: The carbon intensity of energy use \tilde{f} is fit with a piecewise linear function of each region’s cumulative carbon use. By visual inspection, the data on this is grouped into sets separated by the approximate “break point” years $\{1948, 1974\}$ for the tropical region and $\{1953, 1970\}$ for the temperate region. For each such interval the size of the minimum interval in cumulative energy use that contains at least n_{av} data points is computed, where $n_{av} \geq 2$. The data is divided into equal intervals of this length, and a linear fit to the data in each such interval produces a set of estimates \tilde{f}_j at the midpoints \tilde{x}_j of these intervals. A linear fit to this processed data is then computed for each line segment, and the cumulative carbon use at the point where each of the fits is equal to the previous one is computed. Thus, the data itself decides where the break points are, with the approximate input values providing only a starting point for this search. The above-mentioned statistical tests are then run to check that no significant periodicities or nearest neighbor correlations in the residuals. For completeness, this procedure is repeated for earlier $\{\text{tropical, temperate}\}$ approximate break points $\{1862, 1860\}$ corresponding approximately to the first use of oil, and $\{1892, 1914\}$ corresponding respectively to about the time of 1894–95 Berlin conference agreement on colonial divisions and the First World War. However, these earlier fits are not further used in the calculations and are not required to be free of significant periodicities. The point of fitting the data in comparatively small intervals is to avoid the complications of adding and matching periodicity corrections to piecewise continuous fits. The resulting linear fits are sampled as described above.

EMIT: The formulas $\bar{\Theta}_{2J-1} \cos[2\pi N_J j/n] + \bar{\Theta}_{2J} \sin[2\pi(N_J j/n)]$ with values of 1, 2, and 5 for N_J with $1 \leq J \leq 3$ describe periodic corrections to natural logarithms of fossil carbon use for both regions. However, the periodic corrections have larger amplitude than the cases described above and will be included in the source term for the atmospheric carbon balance and thus also the atmospheric heat balance. While the impact of the higher frequency corrections will largely be averaged out in the atmospheric balance integrals, for the lowest frequency correction it is desirable to allow N_1 to be an adjustable parameter. Sampling in this case again uses a rejection method. First, for this case the likelihood of the form described above is integrated analytically over σ and the periodicity amplitudes. For a each of set of values of N_1 between x and $1 + x$ inclusive, where x solves the equation $1 + x = 1/x$, a Hessian approximation to the dependence on the remaining two parameters \bar{E} and ψ is analytically integrated and the result fit with a cubic spline function of N_1 . The fully nonlinear, nearly linear, and linear parameters are then successively sampled as described above.

CARBON: The above atmospheric carbon balance equation given above can be reduced to quadratures to give fractional atmospheric carbon concentration increment $c = c_s S_0 + B S_1 + S_2$ where impact of the initial condition is given by

$S_0 = e^{-\bar{\sigma}(\bar{t}-\bar{t}_s)}$. The integral $S_1 = \bar{\sigma}e^{-\bar{\sigma}\bar{t}} \int_{\bar{t}_s}^{\bar{t}} d\bar{t} e^{\bar{\sigma}\bar{t}} \tilde{F}_{\text{net}} \bar{\beta} / \bar{C}_0$ defines the response to cumulative emissions, and $S_2 = e^{-\bar{\sigma}\bar{t}} \int_{\bar{t}_s}^{\bar{t}} d\bar{t} e^{\bar{\sigma}\bar{t}} \tilde{E}_{\text{net}} \bar{\beta} / \bar{C}_0$ defines the response to the rate of emissions. By approximating historically observed annual and cumulative carbon emissions \tilde{E}_{net} and \tilde{F}_{net} as step functions, this result can be conveniently analytically integrated to give a result that is linear in the initial value c_s and the coefficient \bar{B} . With triennial averaging of the data, no periodic corrections are required in this case. The fully nonlinear and linear parameters are sampled as described above.

HEAT: Taking data far enough back in time that the effect of the difference between the preindustrial base temperature \bar{T}_0 and the initial temperature can be neglected, the above atmospheric heat balance equation can similarly be reduced to quadratures to give $\tilde{T} = \bar{T}_0 + \bar{\mu}e^{-\bar{\alpha}\bar{t}} \int_{\bar{t}_s}^{\bar{t}} d\bar{t} e^{\bar{\alpha}\bar{t}} \ln c$. This result is again linear in two of the three fitting parameters (\bar{T}_0 and $\bar{\mu}$) and also in the amplitudes of the two frequencies of periodic corrections required in this case. In this case it is desirable to let both of the periodic correction frequencies vary, each over the range where the probability density is at least 0.001 times its maximum value.

PROJECT: Taking as input the sets of random samples of modeling parameters obtained as described above, the maximum likelihood result and ninety-nine random samples are projected forward using analytic formulas through carbon emissions, coupled with numerical integration of $d\tilde{E}_{\text{net}}/d\bar{t}$ and the atmospheric carbon and heat balances. To accomplish this, random samples of future carbon intensity of energy production are chosen as described in the text and illustrated in Figure 8. Solutions of the carbon balance constraint of the form given in the text are obtained by integrating between the break points in the slope of carbon intensity vs. cumulative carbon use.

TABLE A.1

Roman Symbols and Functions

Symbol	Meaning
$a = 1/(1 + \exp[-\nu t])$	development index
$b = (h - 1)/h$	decrease/maximum efficiency ratio
$B = \bar{B}/(\bar{\beta}\bar{\sigma})$	near surface carbon saturation
$c = (\tilde{C} - \bar{C}_0)/\bar{C}_0$	fractional CO ₂ concentration increase
C	consumption rate
f	carbon intensity of energy use
$F = K/Y$	αF = capital intensity of production
$F' = dF/da$	derivative of F with respect to a
$G = (\alpha^{-1} - r)K/C$	K/C = capital intensity of consumption
$G' = dG/da$	derivative of G with respect to a
h	fossil/nonfossil efficiency ratio
k	$\beta k K$ is capital for primary energy*
k	f_k fitting time range number
K	total capital
l	$\beta l a$ is labor for primary energy
m	number of different frequencies*
M	number of fitting parameters
$p = 1 + (h - 1)f$	energy production efficiency factor
$r = \bar{r}\bar{t}$	depreciation rate
$t = (\tilde{t} - \bar{t}_0)/\bar{t}$	time
u	cumulative carbon used, with $\dot{u} = \epsilon f w$
$w = p a^\zeta (kK)^\alpha (la)^\omega$	primary energy production rate
$Y = [a^n ((1 - \beta k)K)^\alpha ((1 - \beta l)a)^\omega]^\varphi w^\beta$	production rate is Y/α
$z = 1 - a$	need for development
$\text{AppellF1} = \sum_{m=0}^{\infty} \sum_{n=0}^{\infty} (-a\delta)^m a^n (\psi)_{m+n} (-\alpha/\omega)_m (1)_n / (m!n!(\psi + 1)_{m+n})$	hypergeometric function
$(d)_n = d(d + 1) \dots (d + n - 1)$	rising factorial
$\text{Beta}[x_1, x_2] = \Gamma[x_1]\Gamma[x_2]/\Gamma[x_1 + x_2]$	Euler Beta function
$\mathcal{L} = a^\theta e^{-\rho t} C^{1-\theta} / (1 - \theta) + \kappa \beta a^\theta e^{-\rho t} C^{-\theta}$	$(f w - \dot{u}/\epsilon)$ Lagrangian
\ln	natural logarithm
$\exp[x] = e^x$	exponential function
$S[a] = \int_0^a da a^\psi (1 + a\delta)^{\alpha/\omega} / (za)$	integral for fossil carbon balance

* k and m do not have these meanings when used as subscript integers

TABLE A.2

Subscripted Roman Symbols

Symbol	Meaning
b_θ	constant in wellbeing vs. wealth fit
c_s	initial condition for c
d_1	log-normal distribution sample for f_{break}
d_2	log-normal sample affecting slope after f_{break}
d_3	log-normal sample used with f_{act}
d_2	log-normal sample affecting final slope
f_{act}	most likely second break point for f
$f_{\text{break}} = \text{Max}[0, f_{\text{now}} - (f_{\text{now}} - f_{\text{gas}})d_1]$	first break point for f
f_{gas}	carbon intensity for natural gas
f_{now}	carbon intensity at last fitting point
$f_k = 2\pi k/n$	periodic correction frequencies
$F_1 = (1 + a\delta)/(1 + \delta)$	capitalization lag function approximation
\mathcal{F}_k	periodicity frequencies
m_θ	slope in wellbeing vs. wealth fit
n_{av}	number of points per interval for \tilde{f}_j
n_r	number of depreciation rate data
$n_2 = \lfloor n/2 \rfloor$	$n/2$ rounded down to nearest integer
n_α	number of labor compensation share data
n_θ	number of wellbeing estimates
n_ρ	number of data used for estimating $\bar{\rho}$
N_J	carbon use number of periodic corrections
N_r	dominant Fourier component for \bar{r}
R_α	term in Beta distribution in exponent of α
S_α	term in Beta distribution in exponent of ω
$S_0 = e^{-\bar{\sigma}(\bar{t} - \bar{t}_s)}$	initial condition effect on temperature
$S_1 = \bar{\sigma} e^{-\bar{\sigma}\bar{t}} \int_{\bar{t}_s}^{\bar{t}} d\bar{t} e^{\bar{\sigma}\bar{t}} \tilde{E}_{\text{net}} \bar{\beta} / \bar{C}_0$	temperature response to cumulative CO ₂
$S_2 = e^{-\bar{\sigma}\bar{t}} \int_{\bar{t}_s}^{\bar{t}} d\bar{t} e^{\bar{\sigma}\bar{t}} \tilde{E}_{\text{net}} \bar{\beta} / \bar{C}_0$	temperature response to rate of emissions

TABLE A.3

Roman Symbols with Overbars

Symbol	Units	Meaning
\bar{A}_n	various	periodicity correction amplitude
$\bar{A}_k = (2/n) \sum_{m=1}^n \bar{e}_m \sin[mfk]$	various	sine correction amplitude
$\bar{B}_k = (2/n) \sum_{m=1}^n \bar{e}_m \cos[mfk]$	various	cosine correction amplitude
\bar{B}	(ppm/yr)/EJ	near surface carbon saturation
\bar{C}_0	ppm (by mass)	base level CO ₂ concentration
\bar{D}_m	various	residuals
\bar{e}_m	various	residuals before periodic corrections
\bar{E}	GT/yr	scale factor for carbon burning rate
\bar{f}_k	GT/EJ	carbon intensity intercepts
\bar{k}_ρ	yr ^{-n_ρ-1}	probability integral normalization
\bar{m}_k	1/EJ	carbon intensity slopes
\bar{P}_{base}	billions of people	base year populations
\bar{P}_∞	billions of people	long term populations
\bar{P}_k	various	Fourier power spectrum amplitudes
\bar{r}_j	1/yr	depreciation rate data
$\bar{s}^2 = (1/\nu_\rho) (\sum_{j=1}^n (\tilde{y}_j - \hat{\rho})^2 / \tilde{W}_j^2) n / \sum_{j=1}^n (1 / \tilde{W}_j^2)$	1/yr ²	weighted variance
$\bar{t} = 1/(\bar{r} + \bar{\rho})$	yr	capitalization time
\bar{t}_0	Julian yr	development index inflection time
\bar{t}_s	Julian yr	heat emissions reference time
\bar{t}_S	Julian yr	carbon balance reference time
\bar{T}_0	°C	base for \bar{T} minus reference value
\bar{T}_n	yr	periodicity correction periods
\bar{w}	EJ/yr	sustainable primary energy use rate
$\bar{W}^2 = n / \sum_{j=1}^n (1 / \tilde{W}_j)^2$	1/yr ²	harmonic average of \tilde{W}_j^2

TABLE A.4

Roman Symbols with Overscripts other than Overbars

Symbol	Units	Meaning
\hat{B}	dimensionless	maximum likelihood for B
\tilde{C}	ppm (by mass)	atmospheric CO ₂ concentration
$\tilde{E} = \bar{E}a^\psi f p F_1^{\alpha/\omega}$	GT/yr	carbon burning rate
$\tilde{f}_k = \bar{f}_k - \bar{m}_k \tilde{u}$	GT/EJ	carbon intensity
\tilde{f}_j	GT/EJ	carbon intensity at values \tilde{x}_j of \tilde{u}
\tilde{g}_j	GT/EJ	fractional annual GDP growth rates
$\tilde{E}_{\text{net}} = \eta_{\text{net}} \tilde{E}$	GT/yr	carbon emission rate
\tilde{F}_{net}	GT	cumulative carbon emissions
\tilde{G}_{DP}	k\$US1990PPP	GDP
\hat{m}_θ	dimensionless	maximum likelihood for m_θ
\tilde{P}	billions of people	population
\tilde{r}	1/yr	depreciation rate
\hat{R}	dimensionless	estimator for R_α
$\tilde{\mathfrak{R}}_j$	1/yr	real interest rates
\hat{S}	dimensionless	estimator for S_α
\tilde{t}	Julian yr	time
\hat{t}_0	Julian yr	development inflection time estimator
$\tilde{T} = \bar{\mu} e^{-\bar{\alpha} \tilde{t}} \int_{\tilde{t}_s}^{\tilde{t}} d\tilde{t} e^{\bar{\alpha} \tilde{t}} \ln c$	°C	temperature change
\tilde{u}	GT	cumulative carbon use
\tilde{W}_j	1/yr	weights for interest rates
\tilde{x}_j	GT	midpoints of intervals with n_{av} data
$\tilde{y}_j = \tilde{\mathfrak{R}}_j - \hat{\theta} \tilde{g}_j$	1/yr	elements of the vector $\tilde{\mathbf{y}}$

TABLE A.5

Greek Symbols without Overscripts

Symbol	Meaning
$\alpha = 1 - \omega$	capital fraction
β	energy fraction
$\gamma_1 = (1 - (1 + \xi^{-1})/\theta)$	used to find γ_2
$\gamma_2 = 1 + \xi/\omega + \gamma_1(1 - \xi^{-1})$	second order lag coefficient
Γ	Gamma function with $\Gamma[x + 1] = x\Gamma[x]$
$\delta = \nu\theta\xi$	capitalization lag constant
δ_j	residuals
$\epsilon_k = \bar{w}\bar{t}\bar{m}_k$	carbon depletion rates ϵ
ζ	energy productivity exponent
ζ_k	angles for hypersphere sampling
η	GDP productivity exponent
η_{net}	carbon emitted/burned
θ	intertemporal substitutability inverse
κ	Lagrangian multiplier
$\nu = \bar{\nu}\bar{t}$	development rate
$\nu_{\text{free}} = n - M$	correlation test degrees of freedom
ν_ρ	degrees of freedom for ρ
$\xi = \zeta/\omega$	ratio of exponents
ρ	pure time rate of preference
σ	residuals' standard deviation
σ_B	prior standard deviation for B
σ_{priors}	value for standard deviations σ_{prior}
$\varphi = 1 - \beta$	non-energy fraction of production
$\psi = 1 + \zeta + \alpha\xi$	energy use rate exponent
$\Psi = d \ln \Gamma[x]/dx$	digamma function
ω	labor fraction of production

TABLE A.6

Greek Symbols with Overscripts

Symbol	Units	Meaning
$\bar{\alpha}$	ppm/GT	thermal relaxation coefficient
$\bar{\beta}$	1/yr	converts total carbon to CO ₂ ppm
$\tilde{\Delta T} = \tilde{T} + \bar{T}_0$	1/yr	temperature from reference value
$\bar{\theta}_1$	1/yr	depreciation cosine amplitude
$\bar{\theta}_2$	1/yr	depreciation sine amplitude
$\bar{\vartheta}_1$	1/yr	population growth rate constant
$\bar{\vartheta}_2$	1/yr ²	approximate growth rate slope
$\bar{\Theta}_{2J}$	1/yr	carbon use cosine amplitudes
$\bar{\Theta}_{2J-1}$	1/yr	carbon use sine amplitudes
$\hat{\theta}$	dimensionless	estimator for θ
$\bar{\mu}$	°C/yr	greenhouse effect coefficient
$\bar{\nu}$	1/yr	development rate
$\bar{\rho}$	1/yr	pure time rate of preference
$\hat{\rho} = \left(\sum_{j=1}^n \left(\tilde{y}_j / \tilde{W}_j \right) \right) / \left(\sum_{j=1}^{n_\rho} \left(1 / \tilde{W}_j \right) \right)$	1/yr	maximum likelihood estimator for ρ
$\bar{\sigma}$	1/yr	carbon clearance rate coefficient
$\bar{\sigma}_\rho^2$	GT/yr	variance scale for $\bar{\rho}$
$\bar{\tau}_n$	Julian yr	periodicity phases

Acknowledgments

This work was supported in part by the John D. and Catherine T. MacArthur Foundation Grant 274753000 and U.S. Department of Energy Contract 941452401. Michael Grillot and colleagues at the U.S. Energy Information and Gregg Marland at the Oak Ridge National Laboratory generously provided information on energy statistics. Kathleen Anderson-Conner, Rebecca Osgood, Sheila Roberts, and Matthew Rosenstein provided administrative assistance.

References

- Andronova, N., and Schlesinger, M.: 2001, 'Objective estimation of the probability density function for climate sensitivity,' *J. Geophys. Res.* **106**, 22605–22612.
- Barro, R. and Sala-i-Martin, X.: 1995, *Economic Growth*. McGraw-Hill, New York.
- Bickel, P., and Doksum, K.: 1977, *Mathematical Statistics: Basic Ideas and Selected Topics*. Holden-Day, Oakland.
- Bischoff, C., and Kokkelenberg, E.: 1987, 'Capacity utilization and depreciation rate,' *Applied Economics* **19**, 995–1006.
- Box, G., and Tiao, G.: 1972, *Bayesian Statistical Inference*. Addison-Wesley, Reading, MA.
- Bu, Y.: 2006, 'Fixed capital stock depreciation in developing countries: Some evidence from firm level data,' *The Journal of Development Studies* **45**, 881–901.
- Collins, M., Booth B., Harris, G., Murphy, J., Sexton, D., Webb, M.: 2006, 'Towards quantifying uncertainty in transient climate change,' *Climate Dynamics* **27**, 127–147.
- Darmstadter, J.: 1971, *Energy in the World Economy: A Statistical Review of Trends in Output, Trade, and Consumption since 1925*. Washington, D.C.: Resources for the Future.
- Dessai, S., and Hulme, M.: 2003, 'Does climate policy need probabilities?' Tyndall Centre Working Paper, 34, University of East Anglia, Norwich, UK. Available at <http://www.tyndall.ac.uk/publications/publications.shtml>
- Dessai, S., and Hulme, M.: 2004, 'Climate implications of revised IPCC emissions scenarios, the Kyoto Protocol and quantification of uncertainties' *Integrated Assessment* **2**, 159–170.
- Dettinger, M.: 2006, 'A component-resampling approach for estimating probability distributions from small forecast ensembles,' *Climatic Change* **76**, 149–168.
- Easterly, W., and Rebelo, S.: 1993, 'Fiscal policy and economic growth,' *Journal of Monetary Economics* **32**, 417–458.
- Etemad, B., and Luciani, J.: 1991, *World Energy Production 1800–1985*. Geneva: Droz.
- Forest, C., Stone, P., Sokolov, A., Allen, M., and Webster.: 2002, 'Quantifying uncertainties in climate system properties with the use of recent climate observations,' *Science* **295**, 113–117.
- Füssel, H.: 2007. 'Methodological and empirical flaws in the design and application of simple climate-economy models,' *Climatic Change* DOI 10.1007/s10584-006-9154-y.
- Giorgi F., and Francisco, R.: 2000, 'Evaluating uncertainties in the prediction of regional climate change,' *Geophysical Research Letters* **27**, 1295–1298.
- Giorgi, F.: 2005, 'Climate change prediction,' *Climatic Change*, **73**, 239–265.
- Goldewijk, K.: 2004, HYDE 2.0, History Database of the Global Environment. National Institute of Public Health and the Environment, Netherlands. Accessed at <http://arch.rivm.nl/env/int/hyde> on June 12, 2005; subsequently moved to <http://www.mnp.nl/hyde>
- Gollin, D.: 2002, 'Getting income shares right,' *Journal of Political Economy* **110**, 458–474.

- Greene, A., L. Goddard, L., and Upmanu, L.: 2006, 'Probabilistic multimodel regional temperature change projections,' *Journal of Climate* **19**, 4326-4343.
- Hall, R.: 1988, 'Intertemporal substitution in consumption,' *Journal of Political Economy* **96**, 339-357.
- Hansen, J., Sato, M., Reudy, R., Nazarenko, L., Lacis, A., Lo, K., Schmidt, G., Russell, G., Aleinov, I., Bauer, M., Bauer, S., Bell, N., Cairns, B., Canuto, V., Chandler, M., Cheng, Y., Cohen, A., Del Genio, A., Faluvegi, G., Fleming, E., Friend, A., Hall, T., Jackman, C., Jonas, J., Kelley, Kiang, M., Koch, D., Labow, G., Lerner, J., Menon, S., Miller, R., Novakov, T., Oins, V., Perlwitz, Ja., Perlwitz, Ju., Rind, D., Romanou, A., Shindell, D., Stone, P., Sun, S., Streets, D., Tuasnev, N., Thresher, D., Yao, M., and Zhang, S.: 2006, 'Dangerous human-made interference with climate: 2005, A GISS modelE study,' *Atmospheric Chemistry and Physics Discussions* **6**, 12549-12610.
- Hansen, L., and Singleton, K.: 1996, 'Efficient estimation of linear asset pricing models with moving average errors,' *Journal of Business and Economic Statistics* **14**, 53-68.
- IPCC: 2001, *Climate Change 2001: Mitigation*. Intergovernmental Panel on Climate Change Third Assessment Report, Cambridge University Press, Cambridge.
- Ipsen, D., Rösch, and Scheffran, J.: 2001. 'Cooperation in global climate policy: Potentialities and limitations,' *Energy Policy* **29**, 315-326.
- Jain, A., and Yang, X.: 2005, 'Modeling the effects of two different land cover change data sets on the carbon stocks of plants and soils in concert with CO₂ and climate change,' *Global Geochemical Cycles* **19**, doi:10.1029/2004GB002349.
- Jones, P., Parker, D., Osborn, T., and Briffa, K.: 2001, 'Global and hemispheric temperature anomalies—Land and marine instrumental records. In *Trends: A Compendium of Data on Global Change*, Oak Ridge National Laboratory Carbon Dioxide Information Analysis Center. Accessed at <http://cdiac.ornl.gov/ftp/trends/temp/jonescru/global.dat> on March 14, 2005.
- Keeling, C., and Whorf, T.: 2005, 'Atmospheric CO₂ records from sites in the SIO air sampling network. In *Trends: A Compendium of Data on Global Change*. Carbon Dioxide Information Analysis Center, Oak Ridge National Laboratory, U.S. Department of Energy, Oak Ridge, Tenn., U.S.A. Accessed at <http://cdiac.esd.ornl.gov/ftp/trends/c02/manualoa.co2> on May 21, 2005; subsequently moved to <http://cdiac.esd.ornl.gov/trends/co2/sio-mlo.htm>
- Keller, K., Hall, M., Kim, S., Bradford, D., and Oppenheimer, M.: 2005, 'Avoiding dangerous anthropogenic interference with the climate system,' *Climatic Change* **73**, 227-238.
- Kriegler, E.: 2005, *Imprecise Probability Analysis for Integrated Assessment of Climate Change*. PhD Thesis, Potsdam University, Available at <http://pub.ub.uni-potsdam.de/volltexte/2005/561>
- Kypreos, S.: 2006, 'Stabilizing global temperature change below thresholds: Monte-Carlo Analyses with MERGE-ETL,' Workshop: Cost of Inaction, April 10, Accessed at <http://www.diw.de/english/dasinstitut/abteilungen/evu/aktuelles/index.jsp>
- Maddison, A.: 2001, *The World Economy: A Millennial Perspective*. Organization of Economic Cooperation and Development, Paris.

- Maddison, A.: 2003, *The World Economy: Historical Statistics*. Organization of Economic Cooperation and Development, Paris. Updates available at <http://www.eco.rug.nl/~Maddison>
- Maier-Reimer, E., and Hasselmann, K.: 1987, 'Transport and storage of CO₂ in the ocean—An inorganic ocean-circulation carbon cycle model', *Climate Dynamics* **2**, 6–90.
- Manne, A., Mendelsohn, R., and Richels, R.: 1995, 'MERGE, A model for evaluating regional and global effects of GHG reduction policies,' *Energy Policy* **23**, 17–34.
- Manne, A.: 2006, 'MERGE 5.1. Model for evaluating regional and global effects of GHG reduction policies,' Available at <http://www.stanford.edu/group/MERGE>
- Mitchell B.: 2003, *International Historical Statistics: Africa, Asia, and Oceania, 1750–2000*. New York: Palgrave MacMillan.
- Mastrandrea, M., and Schneider, S.: 2004, 'Probabilistic integrated assessment of "dangerous" climate change,' *Science* **304**, 571–575.
- Murphy, J., Sexton, D., Barnett, D., Jones, G., Webb, M., Collins, M., and Stainforth, D.: 2004, 'Quantification of modelling uncertainties in a large ensemble of climate change simulations,' *Nature* **430**, 768–772.
- Myers, D., and Diener, E.: 1995, 'Who is happy?' *Psychological Science* **6**, 10–19.
- Nakicenovic, N., Alcamo, J., Davis G., de Vries B., Fenhann, J., Gaffin S., Gregory, K., Grübler, A., Jung, T., Kram, T., Lebre La Rovere, E., Michaelis, L., Mori, S., Morita, T., Pepper, W., Pitcher, H., Price, L., Riahi, K., Roehrl, A., Rogner, H., Sankovski, A., Schlesinger, M., Shukla, P., Smith, S., Swart, R., van Rooijen, S., Victor, N., and Zhou D.: 2000, *IPCC Special Report on Emissions Scenarios*. Accessed at <http://www.grida.no/climate/ipcc/emission/index.htm> on January 12, 2007.
- Nehru, V., and Dhareshwar, A.: 1993, 'A new database on physical capital stock: Sources, methodology, and results,' *Revista de Analisis Economico* **8**, 37–59.
- Nordhaus, W.: 1992, 'An optimal transition path for controlling greenhouse gases,' *Science* **258**, 1315–1319.
- Nordhaus, W.: 1993, 'Rolling the DICE: An optimal transition path for controlling greenhouse gases,' *Resource and Energy Economics* **15**, 27–50.
- Nordhaus, W.: 1994, *Managing the Global Commons: The Economics of Climate Change*. MIT Press, Cambridge.
- Nordhaus, W., and Boyer, J.: 2000, *Warming the World: Economic Models of Global Warming*. MIT Press, Cambridge.
- Ogaki, M., and Reinhart, C.: 1998, 'Measuring intertemporal substitution: The role of durable goods,' *The Journal of Political Economy* **106**, 1078–1098.
- Petschel-Held, G., Schellnhuber, H.-J., Bruckner, T., Toth, F., and Hasselmann, K.: 1999, 'Tolerable windows approach: Theoretical and methodological foundations,' *Climatic Change* **41**, 303–331.
- Press, W., Teukolsky, S., Vetterling, W., and Flannery, B.: 1986, *Numerical Recipes in FORTRAN*. Cambridge University Press, Cambridge. Available at <http://library.lanl.gov/numerical/bookpdf.html>
- Raisanen, J., and Ruokolainen, L.: 2006, 'Probabilistic forecasts of near-term climate change based on a resampling ensemble technique,' *Tellus Series a—Dynamic Meteorology and Oceanography* **58** 461–472.

- Ramsey, F. : 1928, 'A mathematical theory of saving,' *Economic Journal* **38**, 543–559.
- Rao, P. K.: 2000, *The Economics of Global Climate Change*. M. E. Sharpe, London.
- Rethinaraj, T.: 2005, *Modeling Global and Regional Energy Futures*. PhD Thesis, University of Illinois at Urbana-Champaign. Text available as an Arms Control, Disarmament, and International Security Program research report at <http://www.acdis.uiuc.edu>.
- Rethinaraj, T., and Singer, C.: 2007, *Historical Energy Statistics: Global and Regional Trends Since Industrialization*. Manuscript in preparation.
- Richels, R., Manne, A., and Wigley, T.: 2004, 'Moving beyond concentrations: The challenge of limiting temperature change,' AEI-Brookings Joint Center for Regulatory Studies, Working Paper 04-11.
- Sachs, Jeffrey: 2005, *The End of Poverty: Economic Possibilities for Our Time*. Penguin, New York.
- Schneider, S., and Lane, J.: 2005, 'Integrated assessment modeling of global climate change: Much has been learned—Still a long and bumpy road ahead' *Integrated Assessment Journal* **5**, 41–75.
- Stainforth, D., Aina, T., Christensen, C., Collins, M., Faull, N., Frame D., Kettleborough, J., Knight ,S., Martin, A., Murphy, J., Piani, C., Sexton, D., Smith, L.A, Spicer, R., Thorpe, A.J, and Allen, M.: 2005, 'Uncertainty in predictions of the climate response to rising levels of greenhouse gases,' *Nature* **433**, 403–406.
- Tol, R.: 1994, 'The damage costs of climate change—a note on tangibles and intangibles, applied to DICE,' *Energy Policy* **22**, 436–438.
- UNSD: 2005, *Energy Statistics 2005*. United Nations Statistics Division, New York.
- Verbeke, T. and De Clercq, M.: 2006. 'The EKC: Some really disturbing Monte Carlo evidence,' *Environmental Modelling and Software*, **21**, 1447–1454.
- WDI: 2005, *World Bank Development Indicators*. Available in electronic format to subscribers at <http://devdata.worldbank.org/dataonline>.
- Webster, M., Babiker, M., Mayer, M., Reilly, J. Harnisch, J., Hyman, R., Sarofim, M., and Wang, C.: 2002, 'Uncertainty in emissions projections for climate models,' *Atmospheric Environment* **36**, 3659–3670.
- Wei, W.: 1990, *Time Series Analysis: Univariate and Multivariate Methods*. Addison-Wesley, Redwood City CA.
- Wolfram, S.: 2003, *The Mathematica Book, 5th Edition*. Wolfram Media, Champaign IL.
- Worrell, E., Ramesohl, S., and Boyd, G.: 2004, 'Advances in energy forecasting models based on engineering economics,' *Annual Review of Environment and Resources* **29**, 345–381.
- Zhang, J.: 2000, *Energy Economic Modeling and Optimization*. PhD Thesis, University of Illinois at Urbana-Champaign.